I am the captain now: The global economic toll of piracy on maritime shipping

July 23, 2024

Renato Molina[1,2*], Juan Carlos Villaseñor-Derbez[3], Gavin McDonald[4,5,6], Grant McDermott[7]

[1]Department of Environmental Science and Policy, University of Miami, Miami
[2]Department of Economics, University of Miami
[3]Oceans Department, Doerr School of Sustainability, Stanford University
[4]Marine Science Institute, University of California, Santa Barbara
[5]Bren School of Environmental Science & Management, University of California, Santa Barbara
[6]Environmental Markets Lab, University of California, Santa Barbara
[7]Department of Economics, University of Oregon

*To whom correspondence should be addressed; E-mail: renato.molina@miami.edu.

Abstract

Modern-day piracy is a pervasive problem for global maritime shipping, yet its economic costs are largely unquantified. We close this knowledge gap by pairing a detailed dataset of global pirate encounters with satellite information of over 25 million shipping voyages. Our empirical analysis identifies the causal impact of piracy on vessel avoidance behavior, forcing longer, safer routes. We estimate increased travel costs of US$1.5 billion annually. Accounting for environmental damages from harmful emissions adds another US$5.1 billion in annual welfare losses. These costs suggest strong support for global anti-piracy policies, with enforcement measures funded at a fraction of current losses.

1 Introduction

Maritime transport is the lifeblood of global economic trade. The oceans carry more than 70% of the world's traded goods by value, and more than 80% by volume (Asariotis et al., 2017). Yet, even as the industry has continued to adapt and prosper, it remains vulnerable to plunder. Piracy grabbed worldwide headlines during the late 2000s after a sharp increase in violent encounters off the coast of Somalia, which culminated in the infamous kidnapping of *MV Maersk Alabama's* Captain Phillips in 2009. The media interest in pirates has since waned, but they remain a major scourge along many global shipping routes. Official global records report more than 2,200 pirate attacks between 2013 and 2021, with over 600 taking place between 2019-2021 alone (see Section 2).

How do these pirate attacks affect shipping behavior and its associated economic outcomes? The answer is *avoidance*. Consider an example from the Makassar Strait in Indonesia, visualized in Figure 1. On June 19, 2013 a Hong Kong-flagged bulk carrier was boarded by pirates. Information on the attack was broadcast to other vessels in the region via the Anti-shipping Activity Messages (ASAM) communication network, allowing them to react.[1] There is a near-total avoidance of the attack area following the ASAM broadcast; the previous cluster of shipping activity near the Muara Jawa Anchorage all but disappeared and was replaced by a new one further South (Panel **A**). The number of voyages in the affected area also dropped from an average of 48 per day to just 3 per day (Panel **B**).

What is the economic impact of shipping vessels avoiding pirates? In this paper, we seek to shed light on this question by merging theoretical insights with rich data on shipping voyages and pirate encounters, which we then use to credibly assess the causal effect of piracy on the shipping industry. Specifically, we develop a formal theory model of sea captains' decision-making process under information uncertainty and the threat of piracy. We then compile a unique geospatial dataset to test our model predictions. The dataset includes high resolution spatio-temporal information on pirate encounters from the US National Geospatial Intelligence

[1] The Worldwide Threat to Shipping Report reads: *On 19 June, the anchored Hong Kong-flagged bulk carrier OCEAN GARNET was boarded at 01-11S 117-12E, at the Muara Jawa Anchorage, Samarinda. Deck watch keepers onboard the anchored bulk carrier noticed three to five robbers with long knives near the forecastle store. They raised the alarm and retreated into the accommodation. On hearing the alarm, the robbers escaped in their waiting boat. Upon investigation, it was discovered that ship's stores had been stolen. Port control was informed.* The entry is available at `https://t.ly/bsNk7` [Last visited on 04/12/24]

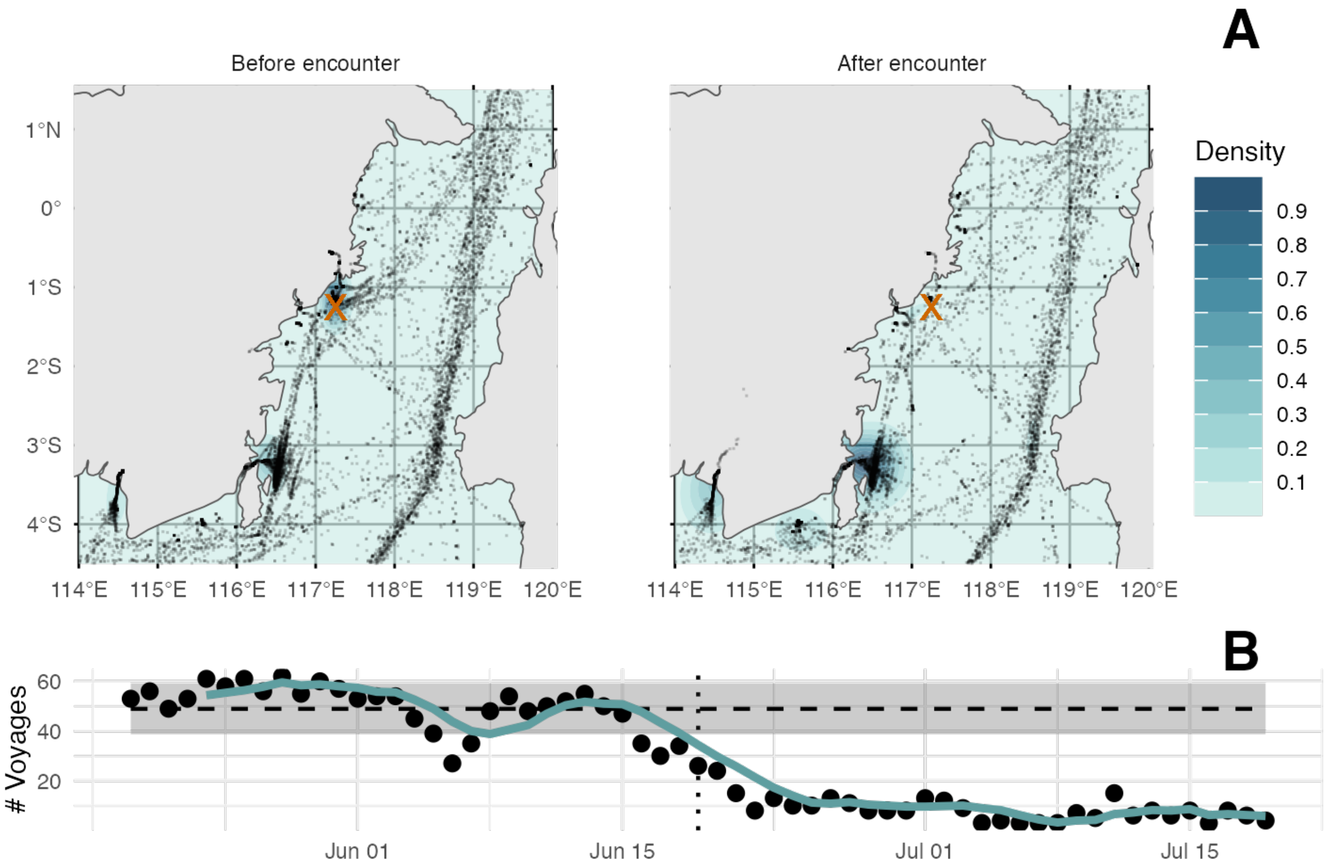

Figure 1: **"X" marks the spot: Example of change in shipping vessel transit following an encounter with pirates on June 19, 2013 off the coast of Indonesia.** Panel **A** shows maps of the Muara Jawa Anchorage before (left) and after (right) the encounter. Small black points show all vessel positions recorded one week before or after the attack, and background colors show a 2-dimensional kernel estimate of vessel density. Panel **B** shows a time series of daily number of voyages crossing the affected pixel (at 117E, 1.5S, indicated with an orange "X" in A). Each point shows the total daily number of voyages, and the blue line shows the mean number in a 5-day rolling window. The horizontal dashed line and shaded area show the baseline number of daily voyages (mean ± standard-deviation) before the attack.

Agency ASAM database,[2] as well as individual vessel tracks of all known cargo, tanker, and refrigerated vessels that use Automatic Identification System (AIS) due to (Kroodsma et al., 2018).

Our empirical results show that a pirate encounter along a shipping route causes vessels to extend their trips by potentially hundreds of kilometers in the months that follow, as they engage in avoidance behavior. When aggregated at the industry level, and taking into account prevailing fuel and labor costs, these adjustments suggest additional transportation costs of about US$1.5 billion as of 2021. Moreover, we estimate that surplus emission of air pollutants (CO_2, NO_x, and SO_x) due to increased fuel usage results in an additional cost of US$5.1 billion in environmental damages. These estimates highlight a considerable previously undocumented loss in terms of operational cost, but also in terms of global fuel consumption and the associated added emissions of both greenhouse gasses and local pollutants.

2 Background

2.1 Piracy and trade

Modern piracy is fundamentally an enforcement problem that can be traced to poorly defined property rights and duties over maritime territory. This misalignment is especially acute in international settings, where the establishment and enforcement of anti-pirate regulations usually conflicts with sovereign rights (Rubin, 1988). These institutional settings reduce the probability of pirates being prosecuted, or even apprehended, which in equilibrium encourages the continued predation of sea commerce.

From a welfare perspective, Anderson (1995) suggests several types of losses associated with piracy. First, direct capital losses due to violence, either in the form of damages to the ship and cargo, or loss of life. Second, indirect losses in the form of resources channeled toward evasion and protection that could have been used for other productive activities. For example, the additional bulk of fuel used to maintain avoidance maneuvers, the cost of hiring and bringing armed personnel on-board, or the additional amount of capital required to sustain a steady flow of goods *vis-á-vis* the same exchanges in the absence of piracy. It follows that

[2] Information reported in The Worldwide Threats to Shipping Report by The Office of Naval Intelligence. Recent reports are available at `https://t.ly/frrm6` [Last checked 04/12/24]

the magnitude of these responses can lead to both intensive and extensive margin adjustments, which in turn can cause dynamic losses in the form of diminished incentives for producers and merchants to continue with or expand production (Anderson, 1995).

Historical data suggest that piracy events have often had extremely negative impacts on commerce channels and local economies. For example, during the seventeenth century, the "Turkish pirates" completely paralyzed several parts of western England (Gray, 1989). Around the same time, the predominance of pirate organizations in the Arabian Sea led to sharp decreases in trade flow, with devastating consequences for industries in the region (Scammell, 1992). These cases are not unique. Similar impacts have been documented in other trade regions such as the Caribbean (Andrews, 1978), the Philippines (Warren, 2007), and Venice (Tenenti, 1967), further illustrating how thriving economies can suffer considerable negative effects when piracy occurs.

Modern piracy has had similar effects and remains a scourge along important trading routes around the world. However, most encounters take place in a few hotspots, namely: the Gulf of Aden (known for the Somali pirates), the Gulf of Guinea (mostly around the Nigerian EEZ), the Malacca Straits (the shipping channel formed by Sumatra and the Malay peninsula) and the South China sea. For the remainder of the paper we will refer to both the Malacca Straits and the South China sea as one group that we call *Southeast Asia*. The distribution of the actual number of encounters in each region over time is shown in Figure 2. From this figure, note that pirate encounters are consistently concentrated in the African region and Southeast Asia.

A relatively sparse literature considers the economic impact of modern piracy. Past estimates suggest that the losses in trade volume due to pirate activities in Somalia accrued to about US$24 billion/year (Burlando et al., 2015). Other estimates are more conservative and suggest that the loss ranged between US$1 billion and US$16 billion, when accounting for the addition of 20 days per voyage due to re-routing around Africa, and increased insurance, charter rates, and inventory costs (Wright, 2008; Bowden et al., 2010; O'Connell and Descovich, 2010). Another estimate suggests that 10 additional hijacks in either the Gulf of Aden or the Strait of Malacca reduce the volume of exports between Asia and Europe by about 11%, with an estimated cost of about US$25 billion per year (Bensassi and Martínez-Zarzoso,

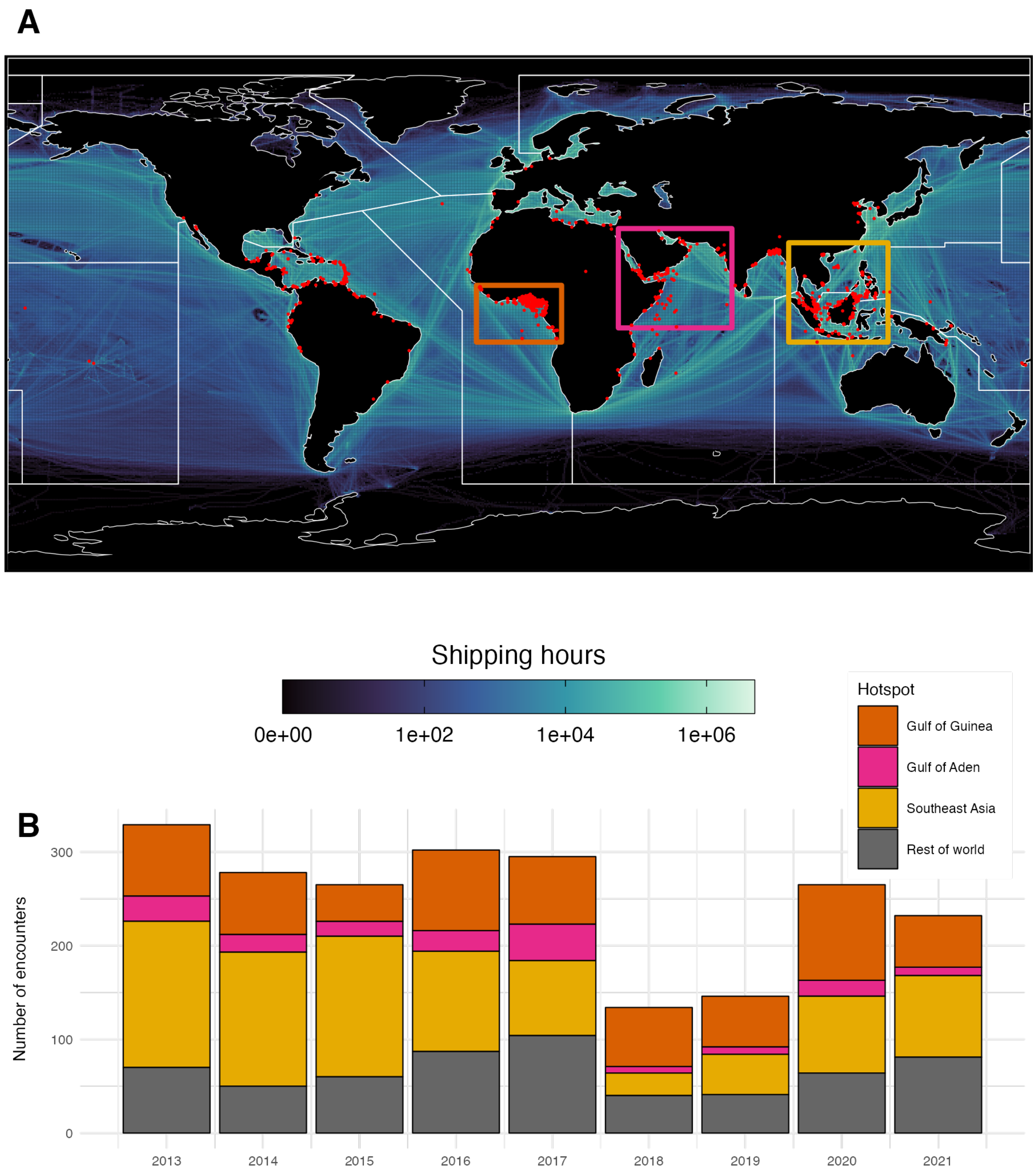

Figure 2: **A global view of modern-day maritime transport and piracy.** Panel **A** shows the spatial overlap of shipping activity and anti-shipping encounters from 2013 to 2021. Note that data are $\log_{10}$-transformed for visualization purposes and represented using a $0.5^{\circ}\times 0.5^{\circ}$ grid in geographic coordinates, with the fill color of each pixel represents the total shipping transit time from 2013-2021 (hr). Pirate encounters are shown as red points. The colored overlay bounding rectangles correspond to the three main piracy hotspots, namely: 1) Gulf of Guinea, 2) Gulf of Aden, and 3) Southeast Asia. The bounding boxes are defined by an empirical density-based clustering approach (see Materials and Methods). Outlines of the major Anti-shipping Activity Messages (ASAM) regions are shown as white lines. Panel **B** shows a number of pirate encounters across hotspots and the rest of the world from 2013 to 2021.

2012). These studies estimate losses through the examination of overall trade patterns, but to the best of our knowledge, there is no study focusing on the behavior of individual shipping vessels. We believe the latter is a more direct and policy-relevant way to disentangle the cost of piracy.

Other empirical settings, including Flückiger and Ludwig (2015) and Axbard (2016), study how poor fishing conditions lead to an increase in pirate activity in Africa and Indonesia, respectively. Studies such as Leeson (2007) and Psarros et al. (2011), consider the factors that contribute to pirates being more or less effective in terms of finding vessels, as well as extracting the most value out of these encounters. Specific to the Somali case, O'Connell and Descovich (2010) and Bahadur (2011a) document the social and economic institutions associated with pirate activities by identifying ransom procedures, operational supply chains, and community support.

Alongside these empirical studies, at least two studies explore the theoretical basis and deterrence implications of piracy. Guha and Guha (2011) model optimal patrolling and penalties under the option of self insurance, while Hallwood and Miceli (2013) explore optimal patrolling and penalties taking into account strategic interactions between pirates and shippers.

Finally, other strains of the literature have devoted themselves to more narrowly-focused aspects of piracy, often from a historical or ethnographic perspective. For example, Anderson (1995) documents the historical evolution of anti-piracy efforts by state and individual actors along shipping routes. Similarly, Liss (2007) describes how modern piracy incentivizes shippers to employ private military companies or acquire their own defense mechanisms.

2.2 The business model of modern piracy

Accurately representing the operational context of piracy is challenging. Pirates typically have little or no incentive to make public the details of their operations. Nonetheless, there are a few credible sources that allow us to establish the mechanics behind pirate encounters, and more importantly, use them as means for identification in the empirical section. We particularly rely on Bahadur (2011b), who conducted a number of first-person interviews with pirate-affiliated individuals in Somalia in the late 2000s.

Per Bahadur (2011b), Somalian pirates do not appear to discriminate between vessels. Instead they opportunistically hijack vulnerable vessels that cross their path. Once the potential target is identified, pirates pursue the vessel until it is out of reach or they eventually capture it. The pirates' search and pursuit are not constrained by the jurisdictional boundaries of Somalia. Their boarding strategy entails splitting into several skiffs, which approach the target vessel from all sides while waving and firing their weapons to scare the ship's crew. If the vessel stops, or the skiffs are able to keep up with it, the pirates then toss rope ladders onto the deck and proceed to board. According to the accounts, crews rarely resist boarding once the pirates successfully get on the deck. Bahadur (2011b) estimates a reported success rate of approximately 20–30%.

Once the pirates successfully take control of the ship, they steer the vessel to a friendly port. At this location, an additional set of guards and translators would board the ship, and ransom negotiations will start. Most ransoms are handled by insurance companies. Upon reaching an agreement, the money is usually delivered via parachute drop-off onto the deck of the ship, and then split amongst the pirates. The amount that each of them would receive is a fixed fraction of the total ransom, and it would vary depending on the task. About half of the pot would go to the actual men boarding the ship, one third to the investors financing the operation, and a sixth to everyone else assisting with logistics and enforcement (Bahadur, 2011b).

The general business model of pirates in our other two "hotspots"—the Gulf of Guinea and Southeast Asia however—appears to differ slightly from that of Somali pirates. For example, pirates in the Gulf of Guinea focus only on kidnapping a subset of crew members for ransom (ICC-IMB, 2018). Another regular practice in this region is the robbery of cargo, especially liquid fuel.[3] For their part, pirate encounters in Southeast Asia appear to involve sophisticated operations targeted at siphoning fuel from tanker vessels.[4] In this type of attack, vessels are also approached and hijacked, but then they are steered towards a siphoning facility on the shore that retrieves the entire cargo. The crew and the ship are usually freed several days after a successful attack (ICC-IMB, 2018).

Finally, pirate encounters have also increased in the Caribbean, especially along the coast

[3] See *Abduction of Crew Off Nigeria Brings Piracy Back to Indian Agenda* by The Wire, available at: `https://t.ly/gVVXJ` [Last Visited on 04/12/24]

[4] See *Pirates in Southeast Asia: The World's Most Dangerous Waters* by Time, available at: `https://t.ly/Ano8q` [Last Visited on 04/12/24]

of Venezuela. Their approach, however, seems to be fundamentally different. Recent reports indicate that coast inhabitants of Venezuela and northern Colombia have been targeting private yachts for small robbery.[5] These encounters are suggested to be sporadic and motivated by the opportunistic predation of groceries and other valuable items that tourists carry. To our knowledge, no hijacks or ransoms for cargo vessels have been reported in this region.

3 A model of pirates and shippers

Having established the institutional and descriptive features of modern piracy, we now develop a formalised model of shipping behavior in the face of piracy. The model that we propose builds on the previous efforts by Guha and Guha (2011) and Hallwood and Miceli (2013), who championed the theoretical understanding of piracy under an economic framework. We specifically highlight the mechanisms behind pirate encounters, and their effect on shipping routes. As we shall show, it follows that all relevant costs associated with piracy can be attributed to deviations from cost-effective behavior in the absence of the threat.

For simplicity, assume only one pirate and one shipper. There is a continuum of paths, $x \in \mathbb{X} = [0, \bar{x}]$, for a certain route. The cost-effective path is given by $x = 0$, while $x = \bar{x}$ represents the most expensive, but feasible, path. One way to think about this characterization is vessels having to sail farther from the coast than is optimal, due to the threat of piracy. The cost of deviating from the optimal path, $c(x)$, is strictly convex in x, and $c(0) = 0$. In the presence of piracy, the shipper chooses the route taking into account the possibility of encountering and being attacked by the pirate.

An encounter might occur when the shipper transits through the area monitored by the pirate, which is given by the segment $x : x = [0, \bar{a})$. Because physical limitations prevent pirates from monitoring all possible transportation paths, it follows that $\bar{a} < \bar{x}$. The probability of an encounter, however, is strictly positive along the $[0, \bar{a})$ interval, and zero everywhere else. This implies that a shipper could reduce the risk of piracy to zero by taking an extremely long path, or by using other transportation methods such a trains or airplanes. Formally, this

[5] See *La piratería regresa al Caribe motivado a la crisis de Venezuela* by El Nacional, available at `https://t.ly/ug40-` [Last Visited 04/12/24]

relationship can be expressed as:

$$\phi(x;\theta)\begin{cases} >0 & ; \quad 0\leq x<\bar{a} \\ =0 & ; \quad \text{Otherwise} \end{cases} \tag{1}$$

with θ being the vector of parameters that characterize the distribution, including $\bar{a}$ and the search effort with which pirates patrol the susceptible waters. The probability function satisfies $\phi_x(x,\theta)<0$ and $\phi_{xx}(x,\theta)>0\;\forall\; x\in[0,\bar{a})$, and $\phi_x(x,\theta)=\phi_{xx}(x,\theta)=0\;\forall\; x\in[\bar{a},\bar{x}]$.

In this model, the pirate decides to attack only after an encounter takes place, in which the shipper loses h. From the pirate's perspective, however, the assault can be either successful (the pirate gets away) or unsuccessful (the pirate gets caught). An attack implies the pirate obtaining a monetary prize or booty, b, which is not necessarily equal to h, and that he cannot determine until the encounter occurs. This assumption implies that the pirate treats b as a randomly distributed variable with cumulative distribution $F(b)$ over support $[0,\bar{b}]$. One way to think about this realization is the assessment of the ship being "worth" pursuing (Bahadur, 2011b).

Before attacking, the pirate assesses the monetary value of the booty with the expected costs of being apprehended with probability, p, and fine, f. As the pirate does not serve time incarcerated,[6] it follows that an attack occurs whenever $b\geq pf$. Therefore, conditional on an encounter, the probability of an attack is given by:

$$\psi(pf)=[1-F(pf)] \tag{2}$$

Finally, the model assumes the shipper cannot observe the patrolling effort of the pirate, but a finite number of paths previously taken for the origin-destiny combination. Denote this history set as $\mathbf{z}=\{z_1,...,z_m\}$ for m different voyages. The shipper also knows which paths have experienced encounters in the past (e.g., through access to the monthly *Worldwide Threat to Shipping* reports published by the Office of Naval Intelligence, or by contracting intelligence firms that provide such information). This complimentary history set is given by $\mathbf{y}=\{y_1,...,y_n\}$, for a total of n encounters. With this information, the shipper can estimate

[6] Guha and Guha (2011) note that a major problem in modern piracy is the lack of credible punishment after aggressors have been apprehended.

the parameters of the encounter probability distribution, including the span of the monitored area, as:

$$\hat{\theta} = \arg\max_{\theta} \{\mathcal{L}(\theta; \mathbf{y}, \mathbf{z})\} \tag{3}$$

with $\mathcal{L}(\theta; \mathbf{y}, \mathbf{z})$ as the likelihood function of $\phi(x, \theta)$. If the market price of the voyage is given by π, it follows that the expected net return for the shipper, R, would be finally given by:

$$R(\pi, x, \hat{\theta}) = \pi - \phi(x, \hat{\theta})\psi(pf)h - c(x) \tag{4}$$

Assuming risk neutrality, it follows that the optimal path is characterized by the proposition below:

Proposition 1. *The optimal path for a shipper in the face of piracy, x^*, depends on the information of past voyages and pirate encounters, $\{\mathbf{y}, \mathbf{z}\}$, and it satisfies:*

$$-\phi_x(x^*, \hat{\theta})\psi(pf)h = c'(x^*) \tag{5}$$

with

$$\hat{\theta} = \arg\max_{\theta} \{\mathcal{L}(\theta; \mathbf{y}, \mathbf{z})\} \tag{6}$$

All proofs are provided in Appendix A.2.

Proposition 1 indicates that the optimal path equalizes marginal expected savings to the marginal cost of deviating from the cost-effective one. The set of feasible optimal paths is then given by the Lemma below:

Lemma 1. *The optimal path for a shipper in the face of piracy is contained in the set $x : x \in (0, \bar{a}]$.*

Lemma 1 suggests two points regarding optimal paths. First, the shipper will never ignore the threat of piracy. Expected losses from encountering and being attacked by a pirate will always be taken into account and thus avoided following the equimarginal principle. Second and consistent with cost minimizing behavior, if the cost of deviating is low enough, total avoidance will never exceed $\bar{a}$. These ideas are illustrated in figure 3, with panel (a) corresponding to interior solutions and panel (b) corresponding total, or maximum, avoidance.

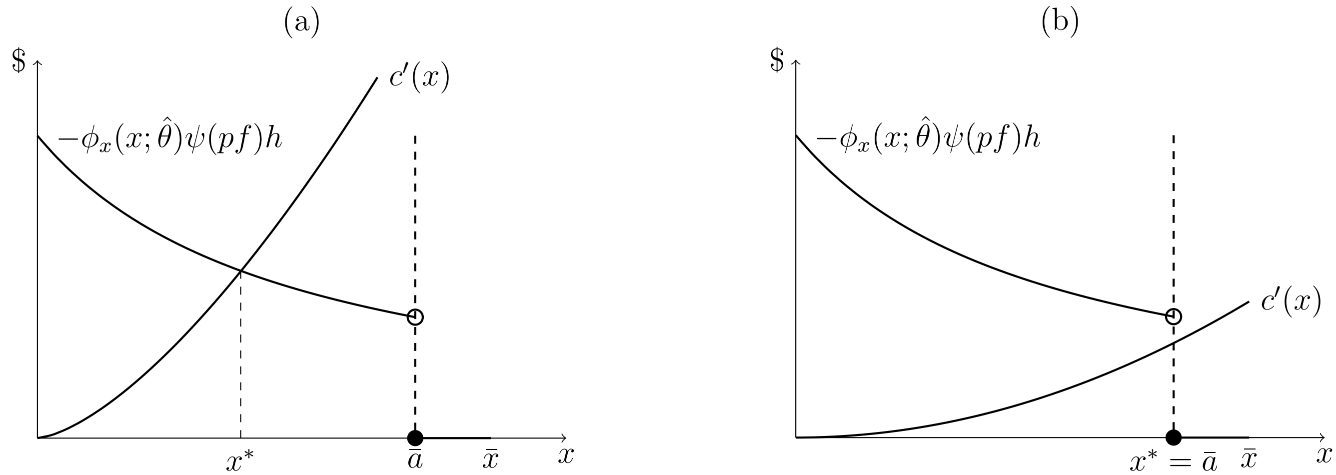

Figure 3: **The shipper's path selection problem.** Panel (a) shows interior solutions, while panel (b) shows the maximum optimal level of avoidance a shipper will ever take when deviating from the cost-effective path is relatively inexpensive.

Now that the shipper's path decision is fully characterized, we turn to establishing the effect of the information set on optimal decisions. In particular, we want to establish how past encounters affect the shippers decision making process today. In line with the empirical analysis, we will focus on the frequency of encounters for path x, which is given by the following ratio:

$$k(x) = \frac{|\mathbf{y} : y_i = x|}{|\mathbf{z} : z_j = x|}; \quad i \in \{1, ..., n\}, j \in \{1, ..., m\} \tag{7}$$

The expected effect of this observable on optimal paths is formalized in the proposition below:

Proposition 2. *The effect of the frequency of encounters, $k(x)$, on optimal path, x^*, is given by:*

$$\frac{\partial x^*}{\partial k(x)} = -\frac{\psi(pf)h\phi_{x\theta}(x^*, \theta)}{\psi(pf)h\phi_{xx}(x^*, \theta) + c''(x^*)} \frac{\partial \hat{\theta}}{\partial k(x)}, \; \forall \, x \in \mathbb{X} \tag{8}$$

Proposition 2 is fairly intuitive: adjustments to optimal paths are linked to their effect in the estimated parameters of the probability function, as well as their effect on the probability of an encounter. In other words, marginal optimal adjustments incorporate any information regarding past encounters along the route to inform the expected probability of encounters. This information is then translated into the adjustments prescribed in Proposition 1. As a Corollary, the sign of this relationship is given by:

Corollary 1. *The direction of the effect of the frequency of encounters, $k(x)$, on optimal path,*

x^*, is given by the sign of the product:

$$-\phi_{x\theta}(x^*, \hat{\theta})\frac{\partial \hat{\theta}}{\partial k(x)} \quad (9)$$

The sign of the above relationship depends on two components: the cross derivative of the probability function, and the effect of observing more encounters along a given route on the estimate of θ. When this expression is positive, it is optimal to deviate more from the cost-effective path, as the increased encounter frequency suggests a higher risk in previously optimal paths. Conversely, if the expression is negative, the optimal deviation decreases, indicating that the observed encounters lead to a lower estimated risk on certain paths. This sign switch is tied to the convexity of the encounter probability function.

To illustrate, suppose encounters are observed farther from the cost-effective path. Operationally, this means an increase in the estimate for $\bar{a}$ and a change in the slopes of the probability function for any x to the left of $\bar{a}$. The actual change will depend on the searching capability of the pirate. Consider the case in which the pirate can allocate only so much time to search every particular section of the feasible paths. The pirate searching farther implies a decrease in the intercept of $-\phi_x(x; \hat{\theta})\psi(pf)h$, or an increase in its slope, or both. Any of these changes effectively reflect a decrease in the probability of encountering the pirate. When this is the case, the intercept with the marginal cost shifts to the left, and thus less avoidance is optimal. Other responses will then be a function of how effective the pirate is when it comes to searching different sections of the path set.

Our main task in the rest of the paper is to establish the above relationship empirically. With this result, we will then be able to price the cost of avoiding pirates. For completeness, however, the characterization of the pirate's behavior is also provided in Appendix A.1.

4 Materials and Methods

Our theoretical model yields three high-level and testable predictions. First, shippers will never ignore the threat of piracy. Second, they will avoid pirates following an assessment of the relative costs of partial and total avoidance, which depends on their potential shipping route(s) and their beliefs about the pirates' capabilities. Third, shippers will incorporate past pirate encounters to inform their avoidance decisions.

With these testable predictions in hand, and to avoid ambiguity, it will prove helpful to define precisely several terms that we use in our empirical analysis. A *route* is a port-to-port combination, a *voyage* is a trip made along a route, and a *path* is the sequence of coordinates chosen by the vessel to travel a route. Similarly, a grid refers to the two-dimensional discretization of geographic space, and a pixel (or grid-cell) refers to a specific two-dimensional bin within the grid.

4.1 Data

We construct a unique dataset for global shipping and piracy that provides both temporal and spatial variation. Specifically, we compile a panel from 2013 to 2021 that includes individual shipping voyages and recent anti-shipping encounters along the route of each voyage. The panel includes the most important operational components that determine the cost of shipping voyages (e.g., engine size, number of crew members, route taken, speed and trip duration) as well as environmental factors affecting it (e.g., wind speed and direction). Data construction assumptions and criteria are described below.

4.1.1 Shipping activity

Individual shipping vessel voyage-tracks come from Automatic Identification System (AIS) data reporting vessel identity, latitude and longitude. AIS transponders are required on all vessels greater than 300 gross registered tons while operating on international voyages, and by many countries while operating in certain exclusive economic zones (McCauley et al., 2016). The dataset from 2013-2021 includes over 100,000 unique known cargo, tanker, and reefer vessels as defined by vessel identification data provided by Global Fishing Watch (GFW) (Kroodsma et al., 2018). We include vessels that are classified as one of *cargo*, *cargo* or *tanker*, *bunker* or *tanker*, *tanker*, *cargo* or *reefer*, *specialized reefer*, *container reefer*, *reefer*, or *bunker*. These vessels broadcast more than 10 billion individual AIS messages during our study period, which we assigned to more than 26 million individual voyages. We leverage GFW's datasets of ports and voyages to assign every single AIS message to a specific port-to-port voyage by a specific vessel (Watch, 2021).

Data on operational costs come from two sources: fuel consumption and labor. We calculate fuel consumption using main engine power, gross tonnage, auxiliary engine power, and design speed. Main engine power and gross tonnage come from GFW's vessel characteristics database (Kroodsma et al., 2018). For each vessel, we determine these characteristics using a hierarchy based on data availability: 1) the official registered information of the vessel; and 2) values inferred by the Global Fishing Watch vessel characteristic neural network when available. Auxiliary power is a function of main engine power, and is calculated using known empirical relationships (Betz, 2011), which link main propulsory requirements with vessel characteristics and auxiliary needs. Design speed is a function of main engine power and gross tonnage (Betz, 2011).

Using these vessel characteristics, we then calculate fuel consumption using a standard approach that combines fuel consumed by both the main and auxiliary engines (Corbett et al., 2009). Fuel consumption of the main engine is defined by hours of operation, main engine power, main engine specific fuel consumption rates (Wang et al., 2007), and a cubic law of operational speed relative to design speed. Fuel consumption of the auxiliary engine is defined by operating hours, auxiliary engine power, and auxiliary engine specific fuel consumption rates (Wang et al., 2007). Fuel consumption is then calculated for each individual AIS ping which are then summed for each voyage.

Daily fuel price data come from Bunker Index. We use the 380 CST Bunker Index, which is the global average price from all ports selling 380 centistoke fuel, the most commonly used fuel in maritime transport. For dates with missing price data, we impute the missing value using the most recent reported price. Most gaps in the data do not exceed more than two days. Total fuel cost for each voyage is then calculated by multiplying the total fuel consumption of the voyage by the fuel price on the date of departure.

We also keep track of labor requirements for individual voyages. Using the ratio suggested in the literature (Betz, 2011), we estimate the crew needed to operate a vessel as a function of its size and type. The crew wage is calculated using the 2018 International Transport Worker's Federation wage scale for the average non-officer seafarer.[7]

We also calculate emissions of CO_2, NO_x, and SO_x for each voyage. CO_2 emissions are calculated using a linear relationship (Corbett et al., 2009), which relies on total fuel consumption

[7]Current and projected wages are available at `https://t.ly/JADDs` [Last Visited on 04/12/24]

of the voyage. SO_x emissions are calculated similarly, under the assumption of 3.3% sulfur content for each kilogram of fuel (Corbett and Fischbeck, 1997). Similarly, NO_x emissions are calculated using a separate conversion rate for both the main engine fuel consumption (which we assume to be a slow-speed engine) and auxiliary engine (which we assume to be a medium-speed engine) (Corbett and Fischbeck, 1997).

Finally, we incorporate a weather proxy in the form of average wind speed and direction along each voyage. We call this proxy the *wind-resistance index.* Wind data come from the National Oceanic and Atmospheric Administration (NOAA) Global Forecast System Atmospheric Model. Mean monthly wind speed and direction information is calculated for $0.5^{\circ}\times0.5^{\circ}$ pixels. We take into account wind direction by decomposing the pitch angle relative to the vessel; the resistance is concave or convex depending on the vessel going against, or with the wind. This measurement is symmetric in absolute terms along each 90° portion of a full circumference, and it goes from 0 to 1. Scaling this measurement by the wind speed gives the final wind-resistance index. For each voyage, the time-weighted mean wind-resistance is then calculated based on the voyage's time spent in each $0.5^{\circ}\times0.5^{\circ}$ pixel.

The final panel covers all global valid cargo and tanker voyages between 2013 and 2021, with each entry reporting vessel characteristics (type, size, crew), departure and arrival dates, departure and arrival ports and countries, total distance traveled (km), time traveled (hr), speed (km/hr), fuel consumption (kg), fuel and labor cost (US$), and emissions (kg).

4.1.2 Pirate encounters

We operationalize pirate encounters using anti-shipping data provided by the United States National Geospatial Intelligence Agency, which includes dates and locations of sightings and hostile acts against ships by pirates, robbers, and other aggressors. We include all reported anti-shipping encounters except those categorized as "Suspicious Approach", as those are not confirmed.[8]

We then divide the ocean into two global grids: one with 0.5° latitude by 0.5° longitude pixels and another with 5° latitude by 5° longitude pixels. The $0.5^{\circ}\times0.5^{\circ}$ grid is used for fine-scale pixel-level analysis, while the $5^{\circ}\times5^{\circ}$ grid is used for port-to-port voyage-level analysis.[9]

[8] This dataset is available at: `https://t.ly/jbmqG` [Last Visited on 04/12/24]

[9] At the equator, a pixel of $5^{\circ}\times5^{\circ}$ is roughly equivalent to 555 km $\times$ 555 km, a reasonable spatial area over

For both datasets, we calculate the number of anti-shipping encounters that occurred in each pixel on each day. This allows us to determine the number of days since the most recent encounter in any given pixel, as well as the number of encounters that occurred within that pixel over a rolling time window. These two panels allow us to conduct analyses at the pixel and voyage levels, respectively.

For the pixel-level analysis, we calculate the number of encounters within rolling windows of the past 3, 6, and 12 months for every $0.5^\circ \times 0.5^\circ$ pixel and every day in the dataset. For the voyage-level analysis, we first calculate the number of encounters within the $5^\circ \times 5^\circ$ pixels along each port-to-port voyage that occurred within a rolling window of the past 3, 6, and 12 months. This provides the number of recent pirate encounters in the area that each voyage passes through and represents, for any given voyage departure date for any given port-to-port route, the captain's expectation of how many encounters they might expect along the route they are about to embark on.

Using the locations of individual anti-shipping encounters that occurred from 2010 through 2021, we also determine hotspots of encounters using density-based clustering as described by (Ester et al., 1996). Implementing a cluster reachability distance of 10 km, and a minimum number of encounters per cluster of 300, we find that attacks correspond to three hotspots of intensive pirate activity for the entire panel: the Gulf of Aden, the Gulf of Guinea, and Southeast Asia. For each of these hotspots we generate a rectangular bounding box that is snapped to the nearest 5° latitude and 5° longitude markers that fully enclose each set of hotspot attacks, and then for each voyage we then determine whether the vessel transited through one or more of these areas.

The final overlap between shipping voyages and pirate encounters, which is the dataset used in the empirical analysis, is shown in Figure 2. Note that pirate encounters concentrate in a few areas in the map. Particularly in the Caribbean, the Gulf of Guinea, the coast of East Africa, the Arabian Sea, and the jurisdictional waters of the Philippines and Malaysia. The relevant hotspots for this study are enclosed by the rectangles.

which shipping vessel operators might make route and speed adjustment decisions in relation to recent anti-shipping encounters. Moving at 10 knots, this is an area that potential attackers could cover in just 30 hours.

4.2 Empirical analysis

4.2.1 Empirical challenges

Establishing the effect of piracy on shipping behavior entails several empirical challenges. One potential problem is the risk of self-selection, whereby pirates target specific ships at the outset of their voyage. It may even be the case that some vessels are actively looking to be hijacked; perhaps due to bribery or infiltration by bad actors. In the presence of such self-selection, our estimates will be affected by omitted variable bias.

According to the documented testimonies described in Section 2.2, most of the initial encounters occur at random. Pirates simply decide to attack after observing the vessel that they happen to run into. The randomness behind these encounters would normally be sufficient for identification, but the presence of sophisticated pirates challenges this claim. In such cases, it is possible that the encounters could actually be planned by pirates or the crew, which implies that they do not occur at random. This issue may be more likely to occur in Southeast Asia, where the attacks appear to be more sophisticated. However, we would argue that the nature of the shipping industry alleviates this concern. The shipping industry operates on a set schedule, regardless of the type of cargo or location. Moreover, these schedules are contracted years in advance (Jansson, 2012; Stopford, 2013) A vessel's departure date is thus pre-determined and plausibly exogenous to pirate encounters in the past. We construct the empirical model around this unique characteristic of both the criminal activity, as well as the shipping industry. Nevertheless, we also supplement the main analysis with an instrumental variable analysis as a robustness check.

Alongside relevant identification considerations, maritime transportation is also highly susceptible to weather conditions. It could be possible that route adjustments after pirate encounters are merely a result of spurious correlation between weather patterns and the timing of past encounters. To account for this possibility, we control for wind patterns along each individual voyage. Wind speed and direction are valid controls for sailing weather conditions as, along with fetch—i,e., area of water over which the wind blows—they determine the size of waves in the ocean (Massel, 2013).

4.2.2 Pixel-level analysis

To establish the effect of piracy on shipping we will rely on several estimation procedures. First, we begin by generally asking if shipping transit is apparently affected by pirate encounters. The analysis is performed under an Eulerian framework, with pixels as the unit of analysis along a 0.5°×0.5° grid. We are specifically interested in how measures of shipping traffic (i.e., total distance traveled within a pixel, total time spent by ships in a pixel, number of voyages and vessels crossing a pixel) change following a pirate encounter.

We extend this analysis with a fixed-effect regression approach connecting pirate encounters and shipping traffic within pixel i at time t. The model takes the following form:

$$y_{it} = \beta TNE_{it} + \gamma' G_i + \theta' X_t + \eta_i + \epsilon_i \tag{10}$$

Here, y is the the measure of shipping traffic, and TNE is the total number of encounters during the past three months, relative to date t. β is the average marginal change related to an additional encounter on mean traffic over a pixel. $\gamma' G_i$ is a vector of fixed effects for the subregion used by the Anti-shipping Activity Messages (ASAM subregion), $\theta' X_t$ captures temporal fixed effects by ASAM region-year-month, while η_i correspond to pixel-specific fixed effects. All of our pixel-level models report standard errors that are robust to spatial heteroskedasticity and autocorrelation with a 100 km cutoff (Conley, 1999). This analysis restricts the sample to pixels with at least one attack during our analysis window (2013-2021; N = 590 pixels). The identification assumption is that the timing and location of past encounters are exogenous to the subsequent shipping traffic after controlling for temporal and pixel-specific fixed effects.

In addition, we estimate dynamic treatment effects by regressing ship traffic on dummy variables indicating relative time (days) to treatment. We include the same suite of fixed effects as per the aggregate effect approach. This ancillary analysis retains only pixels that have at least five days without other encounters before and after the focal encounter date (N = 233 pixels).

4.2.3 Voyage-level analysis

We then analyze the effect of piracy at the voyage level. We are interested in the features of a given voyage i (i.e., distance, duration, and speed) along country-to-country route, r, at time

t, and its performance in terms of operational costs and emissions. The model is as follows:

$$y_{irt} = \alpha + \beta TNE_{rt} + \delta_i VC_i + \lambda_i W_i + \eta_r R_i + \theta' X_t + \epsilon_{irt} \tag{11}$$

where y is the voyage feature and TNE is the total number of encounters during the last three months; the coefficient β thus reflects the average marginal effect of an additional encounter on the mean path of a voyage. VC is a vector of fixed effects according to vessel characteristics (i.e., type of vessel and size), while W is the time-weighted mean wind-resistance index and average wind speed for a given voyage. Finally, R is a vector of fixed effects by route, while X_t is a suite of month by year fixed effects. In the results, we will also control for additional factors such as crossing hotspots, or the voyage being part of the most common port-to-port combination between countries. To account for potential route and temporal correlation, we employ multiway standard error clustering by country-to-country route and year. The identification assumption is that the timing and location of past encounters are exogenous to the date of departure of a given vessel.

4.2.4 Instrumental variables (IV) analysis

In the main analysis, our identification assumption relies on the timing of shipping vessel departures. We assume that these are exogenous to the number of encounters in the preceding months due to shipment schedules. Nonetheless, there is still a chance that sophisticated pirates or shippers might be self-selecting into treatment, thereby violating our exogeneity assumption.

To alleviate these concerns, we conduct an ancillary analysis that relies on an instrumental variables (IV) approach. Here, we will focus on the two hotspots that afflict the African continent, as they are relatively more condensed geographically and follow a similar business model. We conjecture that political stability is correlated with reported pirate encounters within the Economic Exclusive Zones (EEZ) comprising the Gulf of Aden and the Gulf of Guinea, respectively. This is consistent with previous studies on economic stability and the incidence of piracy (Flückiger and Ludwig, 2015; Axbard, 2016). In turn, political stability is only likely to affect a vessel's path through piracy.

Fist, we characterize the Gulf of Aden as the EEZs of Djibouti, Eritrea, Eritrea, Kenya,

Kenya, Oman, Somalia, Tanzania, and Yemen. The Gulf of Aden is characterized by the EEZs of Angola, Benin, Cameroon, Equatorial Guinea, Gabon, Ghana, Liberia, Nigeria, Sao Tome and Principe, Sao Tome and Principe, and Togo. We then count the total number of pirate encounters, and use the observed vessel monitoring data from Global Fishing Watch for our sample of shipping vessels to summarize the total transit time (hr), distance traveled (km), and number of unique vessels that were observed annually in each EEZ from 2013 to 2021.

Next, we take data from the World Bank's Worldwide Development Indicators and track the Political Stability Index by country, which assesses the likelihood of government destabilization or overthrow through unconstitutional or violent means, including terrorism.[10] The index aggregates perceptions from various sources, including surveys and expert evaluations, and ranges from -2.5 (indicating low stability) to 2.5 (high stability).

The analysis is implemented in two stages. The first stage is as follows:

$$TNE_{it} = \Lambda + \Phi PS_{it} + \Psi_i + \Pi' X_t + u_{it} \tag{12}$$

TNE is is the number of encounters, while PS is the reported political stability in country i in year t, respectively. Φ is the marginal change in yearly pirate encounters that follows a change in political stability. Ψ is an indicator variable that takes a value of one if the country belongs to the Gulf of Guinea. X_t is a dummy variable for year t. To account for potential geographical and temporal correlation, we cluster standard errors by hotspot by year.

In the second stage we are interested in the number of vessels that go through EEZ, the distance they travel within EEZs (km/vessel), and the time they spend in said EEZ (hr/vessel), as a function of the pirate encounters in that area. The model is as follows:

$$y_{it} = \alpha + \beta \widehat{TNE}_{it} + \Psi_i + \Pi' X_t + e_{it} \tag{13}$$

y is the shipping measure of interest, while $\widehat{TNE}_{it}$ is the predicted number of encounters in the first stage in country i in year t. To account for potential geographical and temporal

[10]In addition to political stability, the World Bank tracks a variety of indicators that relate to the economic and institutional stability of countries worldwide. These data are updated on a yearly basis and are estimated by country. The data are available online here: `https://t.ly/UbR6y`

correlation, we continue to cluster standard errors by hotspot by year.

5 Results

This section presents the empirical results of the impact of piracy on maritime shipping. It includes pixel- and voyage-level analyses, as well as the supplementary IV analysis at the EEZ level. Summary statistics and supporting tables are provided in Appendix B.

5.1 Empirical evidence of behavioral adjustments by shippers

Our theory model predicts that vessel captains will adjust their paths along a route if they receive new information about the risk of a piracy attack. Just as we saw in Figure 1, this implies that a piracy-afflicted region will receive fewer transits, in expectation, after an attack. We evaluate this prediction empirically by testing for systematic changes in daily transit activity within all $0.5^{\circ} \times 0.5^{\circ}$ pixels that experienced reported pirate activity between 2013 and 2021. The results are displayed in Table 1.

Summarizing, we find that an additional pirate encounter within the preceding 90 days generally leads to a reduction in vessel activity within the affected pixel. This finding holds across a variety of transit measures for all our designated hotspots. For example, a piracy event in the Gulf of Aden correlates to 26.5 fewer kilometers traveled through each pixel within the region during the subsequent three months, as well as 0.7 fewer hours of travel time and 0.65 fewer vessels passing through. The equivalent impacts are less pronounced in magnitude for the Gulf of Guinea and southeast Asia. However, the negative coefficients remain statistically significant for these other two hotspots. The picture is murkier when zooming up to the global level; possibly reflecting a reallocation (spillover) effect between regions and routes that it is difficult to control for. Still, our regional results are robust to a variety of specification and data checks (see Appendix D.1).

Moving beyond pixel-level impacts, how do these adjustments manifest at the level of individual voyages? Bearing in mind the empirical challenges described earlier, we test for changes in core voyage characteristics in Table 2. We observe that a piracy encounter along a vessel's likely voyage path leads to longer average travel distances and prolonged travel times.

Table 1: Effect of Piracy on Pixel-level Ship Transit.

	Global	G. of Aden	G. of Guinea	S.E. Asia
Panel (A): Total Distance (km)				
Encounters (3 mo)	-4.90	-26.50*	-4.58***	-3.69
	(11.53)	(13.78)	(1.32)	(21.18)
Observations	1,939,330	305,691	440,458	489,763
Panel (B): Occupancy (hr)				
Encounters (3 mo)	8.42	-0.70	-0.26	15.97
	(6.73)	(1.20)	(0.62)	(9.89)
Observations	1,939,330	305,691	440,458	489,763
Panel (C): Voyages (#)				
Encounters (3 mo)	0.32	-0.67**	-0.11***	0.79
	(0.44)	(0.34)	(0.04)	(0.68)
Observations	1,939,330	305,691	440,458	489,763
Panel (D): Vessels (#)				
Encounters (3 mo)	0.35	-0.65*	-0.10***	0.83
	(0.45)	(0.34)	(0.04)	(0.69)
Observations	1,939,330	305,691	440,458	489,763

* $p < 0.1$, ** $p < 0.05$, *** $p < 0.01$ The unit of observation is a pixel (N = 590 unique cells). The sample spans from 2013 to 2021. Each panel examines a measure of pixel-level ship transit in terms of total distance in kilometers (km), total occupancy time in hours (hr), and the number of unique voyages or vessels transiting through the pixel. Each column is a different sample: Global is the analysis using the whole sample. G. of Aden, G. of Guinea, and S.E. Asia restrict the sample to cells within each hotspot. Every panel-column combination is a different regression analysis. Encounters (3mo) is the count of pirate encounters recorded within the pixel in the preceding 90 days. All specifications include Fixed-effects by Pixel ID, ASAM Subregion, and ASAM region by year by month. Numbers in parentheses are Conley Standard Errors (100 km cutoff).

The global estimate suggests that an additional pirate encounter within the preceding three months translates to respective increases of 27.83 km in distance and 2.25 hrs in travel time along a given route. We find consistent results when restricting the sample to voyages that traverse hotspots, although the effect again is much more pronounced for voyages passing through the Gulf of Aden (210.9 km and 10.44 hr, respectively).

Table 2: Effect of Past Pirate Encounters on Shipping Voyages.

	Global	G. of Aden	G. of Guinea	S.E. Asia
Panel (A): Total Distance (km)				
Encounters (3 mo)	27.83***	210.90***	26.97***	22.43***
	(3.20)	(19.58)	(1.54)	(3.50)
Panel (B): Total Time (hr)				
Encounters (3 mo)	2.25***	10.44***	1.96***	2.06***
	(0.33)	(0.89)	(0.14)	(0.39)
Panel (C): Average Speed (km/hr)				
Encounters (3 mo)	-0.01*	0.18***	0.04***	-0.02***
	(0.01)	(0.02)	(0.01)	(0.01)
Observations	25,632,233	1,034,377	276,245	6,335,661
Hotspot FE	X	•	•	•

* $p < 0.1$, ** $p < 0.05$, *** $p < 0.01$ The unit of observation is a voyage. Each panel examines an observed feature in terms of total distance in kilometers (km), total time of the voyage in hours (hr), and the average speed of the voyage (km/hr). The sample spans from 2013 to 2021. Every column is a different sample: Global is the analysis using the whole sample. G. of Aden, S.E. Asia, and G. of Guinea restrict the sample to vessels passing through one of the hotspots, respectively. Every panel-column combination is a different regression analysis. Encounters (3mo) is the count of pirate encounters recorded in the projected path of the vessel in the preceding 90 days from the departure date using a 5 degree spatial footprint. Controls include average wind speed along the voyage and the wind-resistance index. Fixed effects include country-to-country combination, vessel type, vessel size, hotspot, and a battery of month by year and top port-to-port combination for country-to-country combination dummies.

In contrast to the economically meaningfully impacts on travel distance and time, the effect on speed is minimal. We interpret these results as an indication that prolonged adjustments to speed are a less cost-effective avoidance measure, or technically infeasible due to engine and vessel limitations. This behavior is consistent with optimal avoidance since the cost of each additional unit of distance traveled grows linearly, while the cost per each additional unit of cruising speed grows exponentially (Wang and Meng, 2012). These results are robust to specification, subsamsampling, and data construction decisions (see Appendix D.2).

Finally, we report our EEZ-based IV analysis in Table 3, which also includes results from a simple ordinary least squares (OLS) regression for reference.[11] The results are consistent with the main analysis. Specifically, travel distance and time per vessel both increase in the presence of piracy. These increases follow our theoretical insights. We note, however, that there also seems to be a significant decrease in shipping EEZ total traffic following pirate encounters after accounting for geographical patterns across hotspots. Contrasted with the OLS analysis, these IV estimates also suggest that failing to account for endogeneity can introduce potential biases. For example, OLS suggests that there are more vessels sailing into these EEZs following a piracy event, whereas the IV estimates show that the relationship is negative.

Table 3: Effect of Yearly Pirate Encounters on EEZ Traffic.

	OLS			**2SLS**		
	(1)	(2)	(3)	(4)	(5)	(6)
Panel (A): Vessels (#)						
Encounters	9.93	9.41	28.25*	-22.01	-24.17	-113.53**
	(12.73)	(10.56)	(13.49)	(37.47)	(36.53)	(48.67)
Panel (B): Distance (km/vessel)						
Encounters	19.03**	19.60**	23.98**	83.26**	83.33**	52.01**
	(7.18)	(7.01)	(8.33)	(30.33)	(31.12)	(18.79)
Panel (C): Time (hr/vessel)						
Encounters	1.45***	1.51***	1.65***	4.59***	4.60***	3.41***
	(0.23)	(0.23)	(0.28)	(1.26)	(1.28)	(0.80)
Gulf of Guinea Dummy			X			X
Year FE		X	X		X	X
F-Stat				25.73	25.56	46.20

* $p < 0.1$, ** $p < 0.05$, *** $p < 0.01$ The unit of observation is a country. Each panel examines an observed feature in terms of total number of vessels transiting an EEZ (#), total normalized distance traveled within an EEZ (hr/vessel), and total normalized time spent within an EEZ (hr/vessel). The explanatory variable is number of pirate encounters. The sample spans from 2013 to 2021. Columns (1) to (3) present the results of ordinary least squares (OLS), while columns (4) to (5) present the result from a two-stage least squares using political stability as an instrument for pirate encounters, respectively. Every panel-column combination is a different regression analysis. Additional covariates include a dummy variable if a country belongs to the Gulf of Guinea and yearly dummies. Standard errors are clustered by gulf by year. Number of observations is 180.

[11] The detailed first-stage results are reported in B.4 in the appendix.

In tandem with the previous regressions, these results all tell a cohesive story: captains are aware of the risk that pirates represent and adjust their paths accordingly. Increases in operational cost and emissions follow directly from these adjustments, and are estimated below.

5.2 The private and public costs of modern-day piracy

Having established robust empirical evidence about the statistical and directional impacts of piracy encounters, we now consider their economic impact. Put simply, how much does the avoidance behavior of vessels cost in monetary terms? We answer this question by using vessel characteristics to determine fuel and labor requirements along a given voyage, and then empirically estimate changes in operational costs at the voyage level. The regression results in table format are available in Appendix B and, consistent with our other findings, suggest that an additional pirate encounter during the preceding three months translates to an average increase of US$830 in input costs (comprising US$580 in fuel and US$260 in labor). While this estimate remains largely consistent across data samples, again we observe a considerably larger effect in the Gulf of Aden. Specifically, our estimates suggest that the marginal effect of a pirate encounter to be over US$5,000 in terms of fuel and over US$1,000 in terms of labor. This discrepancy is striking and it likely reflects the margins of adjustments that captains would pursue while transiting different shipping routes.

We next explore how avoidance actions translate to emissions by establishing the link between pirate encounters and additional CO_2, NO_x and SO_x emissions by shipping vessels. The regression results are provided in Appendix B. Overall, it follows that excessive fuel consumption leads to concomitant emissions across the spectrum of related pollutants. We estimate that a single pirate encounter leads to an approximate increase of 4 tons of CO_2, 85 kg of NO_x, and 70 kg of SO_x per voyage, respectively. NO_x and SO_x excess emissions are relatively less voluminous, though this is a direct consequence of their smaller concentrations in bunker fuel relative to carbon. Once again, limiting the analysis to the Gulf of Aden suggests impacts that are an order of magnitude larger.

To contextualize the practical significance of these estimates, we contrast the implied operational and pollution costs of avoidance behavior during our full 2013–2021 sample with a counterfactual scenario that is absent any pirate activity at the global level. Figure 4 maps the average annual costs to the shipping industry (fuel and labor costs), and additional emission of air pollutants. To monetize these impacts, we use the social cost of each pollutant (Interagency Working Group on Social Cost of Greenhouse Gases [United States Government], 2021; Mier et al., 2021) and derive an aggregate measure of the global costs of piracy that averages US$6.6 billion/year. This figure corresponds to about 1.95% of the total private and public cost generated by the shipping sector in our sample. Approximately US$1.5 billion of this topline number is attributable to private operational costs like fuel and labor, while US$5.1 billion is attributable to public damages (due to air pollution). Overall, 86.4% of the costs of air pollutants occur within a nation's EEZ (200 NM; covering just $\tilde{1}/3$ of the ocean's surface), and 24.7% occur within a nation's territorial seas (12 NM). ASAM regions 7 and 9 (containing the Southeast Asian hotspot) account for US$2.8 billion and US$1.9 billion, ASAM region 6 (containing the Gulf of Aden) accounts for US$643 million, and ASAM region 5 (Gulf of Guinea) accounts for US$623 million. The results underlying Figure 4 are reported in detail in Appendix C.

6 Discussion

This paper examines the effect of piracy on the shipping industry. We document the mechanisms through which shippers adjust their behavior in response to reported pirate encounters along a route, and the implied costs of shipping delays and environmental damages. While our estimated adjustments may seem relatively small at the individual level, cumulatively they translate to a significant economic welfare loss in the aggregate. Taking the total flow of global shipping routes into account, we find that piracy avoidance is a considerable cost to the shipping industry, as well as an overlooked source of environmental externalities.

The economic theory underlying our analysis suggests that ships optimally adjust to reduce the probability of pirate encounters. But those adjustments do not necessarily mean a complete change of routes (i.e., start and end points remain the same). This intuition holds up well in the data, where we observe ships traveling longer voyages, albeit at the cost of higher fuel consumption and labor time. Each additional encounter amplifies this behavioral response, and the effects have long-term implications after a single encounter is reported.

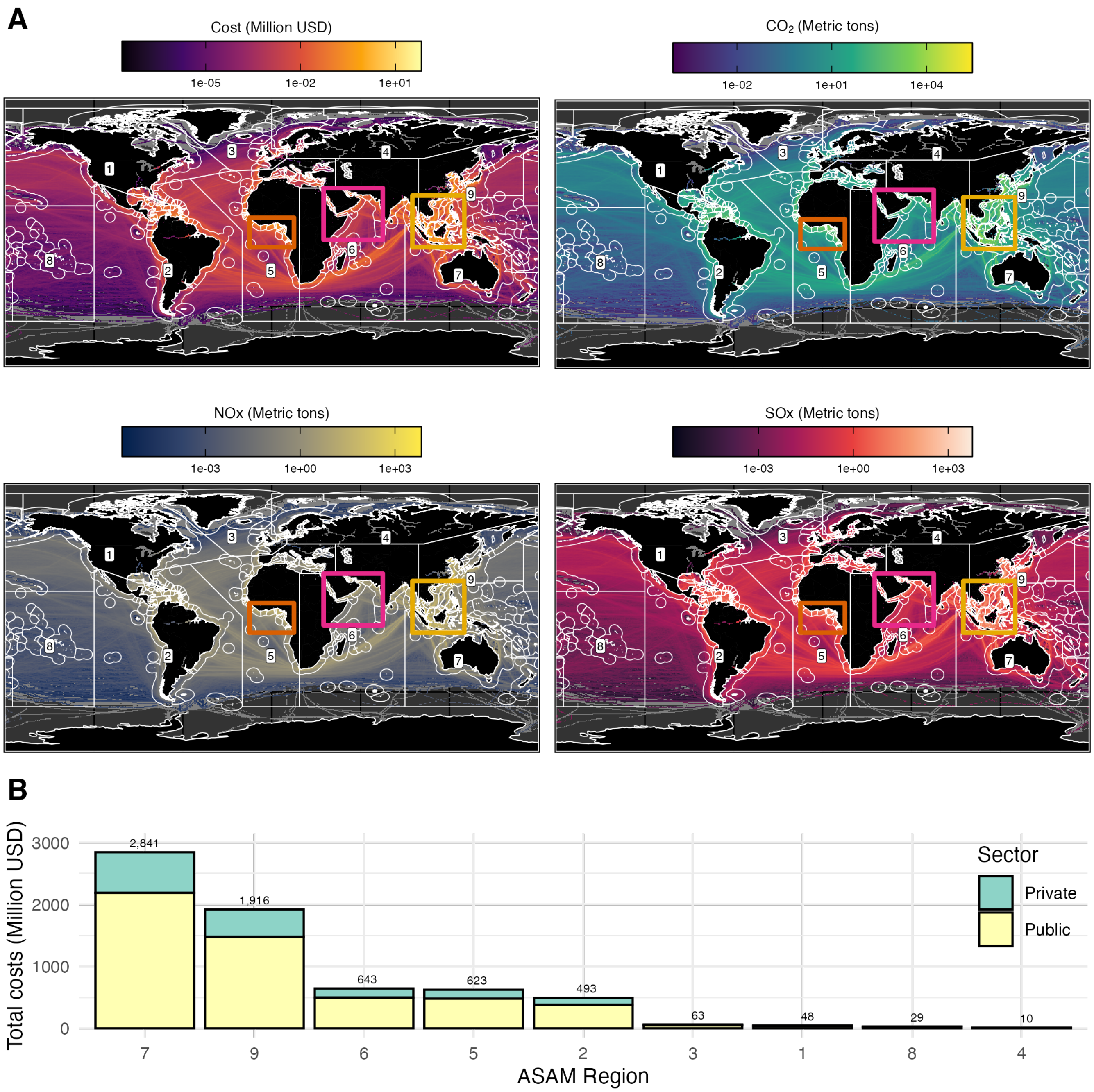

Figure 4: **Additional Operational Costs and Emissions due to Piracy.** Panel **A** shows maps of mean annual private costs to shippers (labor and fuel costs; Million USD), and additional CO_2, NO_x, and SO_x emissions (Metric tons). Nation's Exclusive Economic Zones and ASAM regions are shown in white. White labels indicate ASAM region codes. Note that data are $\log_{10}$-transformed for visualization purposes and represented using a $0.5° \times 0.5°$ grid in geographic coordinates. Panel **B** shows the total costs (Million USD) associated with piracy by ASAM region, where we sum private costs to shippers as well as the cost of damages imposed by additional emissions based on the social-cost of each pollutant.

As we have tried to emphasize, the Gulf of Aden is something of an anomaly in our empirical results, yielding effects that are up to an order of magnitude larger even than other piracy hotspots. Why would the Gulf of Aden present such a different level of adjustment? One potential explanation is that Somali pirates have achieved special notoriety due to past intense media coverage and portrayals. But it could also reflect the geographical characteristics of the region, which allows larger margins of adjustment for a given route. For example, vessels destined for Europe can decide between going through the Gulf of Aden and crossing through Egypt, or circling around the Cape of Good Hope. All vessels going to Nigeria must go through the Gulf of Guinea hotspot. As suggested by our theory, the way in which captains assess the relative piracy risk of following a given path and the potential cost of doing so in different regions affects the magnitude of their adaptation.

We note a few caveats. The first and most important to our causal identification, is the assumption that prior pirate encounters occur at random, relative to the date of departure of a given voyage. This assumption seems to hold in many instances, but some of the documented cases put the randomness assumption into question. In particular, hijacks that target certain types of ships, or the possibility of encounters targeting one particular vessel or poorly-enforced ports and anchorages. We control for all available observables, and use the nature of shipping contracts to minimize the risk of presenting biased results. Given the robustness of our results across a suite of model specifications (Appendix D) and the results from an auxiliary IV analysis, we believe that we have minimized the potential for these issues.

Such caveats notwithstanding, we emphasize that the effects of piracy are clear and consistent across our analysis. Our results not only highlight how problematic piracy is for the shipping industry, specifically, but also underscore a set of wider impacts that ripple across the global economy. We can posit several channels through which these wider impacts manifest. The first channel is a simple waste of capital. Because individual shippers implement avoidance measures to reduce the probability of an encounter, they must allocate capital to cover these actions. Such capital could have been used somewhere else, either in the form of additional voyages, or as an input to other productive activities.

A second channel is environmental impacts. The adjustments to piracy are not emission-neutral. In the aggregate, maritime commerce remains as one of the most emission-intense forms of transportation, with direct contributions to both global greenhouse emissions and local air pollutants that may disproportionately affect different areas and populations (Corbett and Fischbeck, 1997). Our calculations of additional emission burdens shed some light on these potential effects, and highlight how piracy may indirectly result in significant and harmful increases in emissions globally.

A third channel for wider economic impacts is the potential for indirect trade costs. Depending on the level of competitiveness of the affected industry, and the routes in question, the associated costs in transportation could simultaneously affect both producers and consumers. Previous studies have explored this problem using a trade framework (Bensassi and Martínez-Zarzoso, 2012; Burlando et al., 2015), and we believe that our approach of examining individual voyages helps further clarify the mechanism behind previously estimated trade effects, both at a local and a global scale. Further investigation of this issue could unveil important implications for developing legislation that ensures maritime security and fluid trade between nations.

Stepping back, three key insights derive from our results. First, the piracy problem remains prevalent at a global scale. Second, because of the volume of voyages associated with the shipping industry, individual avoidance behaviors accumulate into an economically meaningful loss in aggregate welfare. These losses not only reflect the direct impact on trade flows and transportation inputs (e.g., fuel costs), but also the indirect environmental costs from pollution. Third, our results highlight the value of enforcement and anti-piracy measures for piracy-prone areas. According to available public data (Sonnenberg, 2012), a cost-effective defense task could be deployed for roughly US$330M/year (adjusted for inflation). Enforcement spending would thus cost only a fraction of the total value currently lost due to piracy, and could help reduce large private and public costs (Sonnenberg, 2012). Potentially addressing this gaps in enforcement will require active cooperation from multiple sectors and nations. The benefits, however, can be enjoyed widely.

Finally, an important angle of this issue relates to tackling the roots of the piracy problem in the developing world: poverty. Partnerships involving both public and private participation could potentially prove highly cost-effective and generate benefits at a large scale. Studying the design and implementation of such policies is a promising area for future research.

Competing interests

The authors declare no competing interests.

References

Anderson, John L. 1995. Piracy and world history: An economic perspective on maritime predation. *Journal of World History* : 175–199.

Andrews, Kenneth R. 1978. *The Spanish Caribbean: trade and plunder, 1530-1630.* Yale University Press New Haven.

Asariotis, Regina, Mark Assaf, Hassiba Benamara, Marco Fugazza, Jan Hoffmann, Anila Premti, Luisa Rodriguez, et al. 2017. Review of maritime transport, 2017. Technical report, United Nations Conference on Trade and Development.

Axbard, Sebastian. 2016. Income opportunities and sea piracy in indonesia: Evidence from satellite data. *American Economic Journal: Applied Economics* 8 (2): 154–94.

Bahadur, Jay. 2011a. Deadly waters. inside the hidden world of somalia's pirates. In *US Naval Institute Proceedings*, volume 137. 73–74.

———. 2011b. *The pirates of Somalia: Inside their hidden world.* Vintage.

Bensassi, Sami, and Inmaculada Martínez-Zarzoso. 2012. How costly is modern maritime piracy to the international community? *Review of International Economics* 20 (5): 869–883.

Betz, Sarah. 2011. Reducing the risk of vessel strikes to endangered whales in the santa barbara channel. Ph.D. thesis, University of California, Santa Barbara.

Bowden, Anna, Kaija Hurlburt, Eamon Aloyo, Charles Marts, and Andrew Lee. 2010. *The economic costs of maritime piracy.* One Earth Future Foundation.

Burlando, Alfredo, Anca D Cristea, and Logan M Lee. 2015. The trade consequences of maritime insecurity: evidence from somali piracy. *Review of International Economics* 23 (3): 525–557.

Conley, Timothy G. 1999. Gmm estimation with cross sectional dependence. *Journal of econometrics* 92 (1): 1–45.

Corbett, James J, and Paul Fischbeck. 1997. Emissions from ships. *Science* 278 (5339): 823–824.

Corbett, James J, Haifeng Wang, and James J Winebrake. 2009. The effectiveness and costs of speed reductions on emissions from international shipping. *Transportation Research Part D: Transport and Environment* 14 (8): 593–598.

Ester, Martin, Hans-Peter Kriegel, Jörg Sander, Xiaowei Xu, et al. 1996. A density-based algorithm for discovering clusters in large spatial databases with noise. In *Kdd*, volume 96. 226–231.

Flückiger, Matthias, and Markus Ludwig. 2015. Economic shocks in the fisheries sector and maritime piracy. *Journal of Development Economics* 114: 107–125.

Gray, Todd. 1989. Turkish piracy and early stuart devon. *Reports of the Transactions of the Devonshire Association for the Advancement of Science* 121: 161.

Guha, Brishti, and Ashok S Guha. 2011. Pirates and traders: Some economics of pirate-infested seas. *Economics letters* 111 (2): 147–150.

Hallwood, Paul, and Thomas J Miceli. 2013. An economic analysis of maritime piracy and its control. *Scottish Journal of Political Economy* 60 (4): 343–359.

ICC-IMB. 2018. Piracy and armed robbery against ships: Report for the period 1 january - 31 december 2017. Technical report, International Maritime Bureau of the International Chamber of Commerce.

Interagency Working Group on Social Cost of Greenhouse Gases [United States Government]. 2021. Technical support document: Social cost of carbon, methane, and nitrous oxide interim estimates under executive order 13990. Online.

Jansson, Jan. 2012. *Liner shipping economics.* Springer Science & Business Media.

Kroodsma, David A, Juan Mayorga, Timothy Hochberg, Nathan A Miller, Kristina Boerder, Francesco Ferretti, Alex Wilson, et al. 2018. Tracking the global footprint of fisheries. *Science* 359 (6378): 904–908.

Leeson, Peter T. 2007. An-arrgh-chy: The law and economics of pirate organization. *Journal of political economy* 115 (6): 1049–1094.

Liss, Carolin. 2007. Privatization of maritime security in southeast asia. In *Private Military and Security Companies*. Springer, 135–148.

Massel, Stanislaw R. 2013. *Ocean surface waves: their physics and prediction*, volume 36. World scientific.

McCauley, Douglas J, Paul Woods, Brian Sullivan, Bjorn Bergman, Caroline Jablonicky, Aaron Roan, Michael Hirshfield, et al. 2016. Ending hide and seek at sea. *Science* 351 (6278): 1148–1150.

Mier, Mathias, Jacqueline Adelowo, and Christoph Weissbart. 2021. Taxation of carbon emissions and local air pollution in intertemporal optimization frameworks with social and private discount rates.

O'Connell, Ryan J, and Christopher M Descovich. 2010. Decreasing variance in response time to singular incidents of piracy in the horn of africa area of operation. Technical report, Naval Postgraduate School Monterey CA Department of Information Sciences.

Psarros, George Ad, Alexander F Christiansen, Rolf Skjong, and Gjermund Gravir. 2011. On the success rates of maritime piracy attacks. *Journal of transportation security* 4 (4): 309.

Rubin, Alfred P. 1988. Law of piracy, the. *Int'l L. Stud. Ser. US Naval War Col.* 63: 13.

Scammell, Geoffrey Vaughn. 1992. European exiles, renegades and outlaws and the maritime economy of asia c. 1500–1750. *Modern Asian Studies* 26 (4): 641–661.

Sonnenberg, Dirk C. 2012. Maritime law enforcement a critical capability for the navy. Ph.D. thesis, Monterey, California. Naval Postgraduate School.

Stopford, Martin. 2013. *Maritime economics.* Routledge.

Tenenti, Alberto. 1967. *Piracy and the Decline of Venice, 1580-1615*. Univ of California Press.

Wang, Chengfeng, James J Corbett, and Jeremy Firestone. 2007. Modeling energy use and emissions from north american shipping: application of the ship traffic, energy, and environment model. *Environmental science & technology* 41 (9): 3226–3232.

Wang, Shuaian, and Qiang Meng. 2012. Sailing speed optimization for container ships in a liner shipping network. *Transportation Research Part E: Logistics and Transportation Review* 48 (3): 701–714.

Warren, James Francis. 2007. *The Sulu Zone, 1768-1898: The dynamics of external trade, slavery, and ethnicity in the transformation of a Southeast Asian maritime state*. NUS Press.

Watch, Global Fishing. 2021. Anchorages, ports and voyages data.

Wright, R. 2008. Piracy set to escalate shipping costs. *Financial Times, November* 20.

Appendix for:
I am the captain now: The global economic toll of piracy on maritime shipping

A Additional theory and proofs

A.1 Optimal pirate behavior

In this section, we expand the theoretical insights of the main model to include the behavior of the pirate when deciding on how intensely to search for the target vessels. The working assumption of the model was that the pirate encounters occur whenever $b \geq pf$. The expected value of a successful encounter is then given by:

$$G(pf) = \int_{pf}^{\bar{b}} (b - pf) dF(b) \tag{A.1}$$

In this model, the pirate cannot directly observe the routing of the shipper, but he can still build an estimate. This estimate follows from observing past encounters, $\mathbf{y} = \{y_{(1)}, ..., y_{(n)}\}$, and its own search effort, θ. Further, the pirate knows the probability of an encounter is given by $\phi(x, \theta)$. He is then able to estimate the path of the shipper and the associated probability of an encounter as:

$$\hat{x} = \arg\max_x \{\mathcal{L}(x; \theta, \mathbf{y})\} \tag{A.2}$$

with $\mathcal{L}(x; \theta, \mathbf{y})$ as the likelihood function of $\phi(x; \theta)$. If the pirate has a search cost $s(\theta)$, which is increasing in $\bar{a}$, the expected return to piracy is then given by:

$$R^p(\theta) = G(pf)\phi(\hat{x}, \theta) - s(\theta) \tag{A.3}$$

In addition, the pirate has a total time constraint, $h = b + t(\theta)$, with b denoting the time working in non-pirate activities for wage w. $t(\theta)$ is a function that denotes the total time devoted to searching for vessels. The pirate's concave utility of income is then given by:

$$u(m, \theta) = wb + R^p(\theta) \tag{A.4}$$

The time constraint can be rearranged as:

$$b = h - t(\theta) \tag{A.5}$$

and the utility function can be solely expressed as a function of θ as:

$$u(m, \theta) = w(h - t(\theta)) + R^p(\theta) \tag{A.6}$$

Taking partials with respect to θ and equalizing to zero gives:

$$-u'(\bullet)(bt'(\theta) + G(pf)\phi_\theta(\hat{x}, \theta) = 0 \tag{A.7}$$

This expression defines optimal set adjustments for the pirate, which are captured by θ^*, and implicitly defined by:

$$\phi_{\theta^*}(\hat{x}, \theta^*) = \frac{bt'(\theta^*)}{G(pf)} \tag{A.8}$$

This expression suggests that optimal pirate effort equates the marginal expected gain of increasing the probability of an encounter with the marginal opportunity cost of working in non-pirate activities. Following the same approach as with the shipper, it is straight forward to show that the optimal pirate response to changes in the estimated path are given by:

$$\frac{\partial \theta^*}{\partial \hat{x}} = -\frac{\phi_{x\theta}(\hat{x}, \theta^*)}{\phi_{\theta\theta}(\hat{x}, \theta^*) - \frac{b}{G(pf)} t''(\theta)} \tag{A.9}$$

Our setting does not allow to sign the above expression. Nonetheless, with a few assumptions regarding both the probability and the time requirement function, clear predictions associated with the pirate behavior in the face of different observables are possible.

A.2 Proofs

A.2.1 Proposition 1

Proof. The shipper's problem is given by:

$$\max_{x}\{\pi - \phi(x,\hat{\theta})\psi(pf)h - c(x)\} \tag{A.10}$$

Taking partials with respect to x and equalizing to zero:

$$-\phi_x(x,\hat{\theta})\psi(pf)h - c'(x) = 0 \tag{A.11}$$

Rearranging and multiplying by minus one:

$$-\phi_x(x^*,\hat{\theta})\psi(pf)h = c'(x^*) \tag{A.12}$$

Finally, $\hat{\theta}$ is estimated by examining the sequence of where past encounters took place, $\mathbf{y} = \{y_1, ..., y_n\}$, as:

$$\hat{\theta} = \arg\max_{\theta}\{\mathcal{L}(\theta; \mathbf{y}, \mathbf{z})\} \tag{A.13}$$

These two equations define the optimal path for the shipper based on past encounters, and complete the proof. □

A.2.2 Lemma 1

Proof. First, consider the case of zero avoidance, or $x^* = 0$. From the shipper's problem we know that optimal deviation must satisfy:

$$\phi_x(x,\hat{\theta})\psi(pf)h = -c'(x) \tag{A.14}$$

Because $c(x)$ is convex and $c(0) = 0$, it follows that $c'(0) = 0$. Substituting into the optimality condition then gives:

$$\phi_x(0,\hat{\theta}) = 0 \tag{A.15}$$

which is equivalent to say that the only possibility for x to be equal to zero is if $\phi_x(0,\theta) = 0$, which is never true by design.

Second, consider the case of total avoidance, or $x^* \geq \bar{a}$. Recall that

$$\phi_x(x,\theta) = 0 \ ; \ \forall\, x \geq \bar{a} \tag{A.16}$$

This condition implies that any deviation beyond $\bar{a}$ renders no further reduction in the probability of an encounter. Because of the convexity of $c(x)$, it follows that any $x > \bar{a}$ is strictly inferior to $x = \bar{a}$. Therefore, if $\nexists\, x \in [0,\bar{a}) : \phi_x(x,\hat{\theta})\psi(pf)h = -c'(x)$, optimal decision making dictates $x^* = \bar{a}$. All other scenarios are described by the optimality condition, which completes the proof. □

A.2.3 Proposition 2

Proof. Consider the optimality condition:

$$-\phi_x(x^*, \hat{\theta})\psi(pf)h = c'(x^*) \tag{A.17}$$

Totally differentiating with respect to $k(x)$ gives:

$$-\psi(pf)h\left(\phi_{xx}(x^*, \hat{\theta})\frac{\partial x^*}{\partial k(x)} + \phi_{x\theta}(x^*, \hat{\theta})\frac{\partial \hat{\theta}}{\partial k(x)}\right) = c''(x^*)\frac{\partial x^*}{\partial k(x)} \tag{A.18}$$

Rearranging with the respect to the partial effect on optimal routing x^*:

$$\frac{\partial x^*}{\partial k(x)} = -\frac{\psi(pf)h\phi_{x\theta}(x^*, \hat{\theta})}{\psi(pf)h\phi_{xx}(x^*, \hat{\theta}) + c''(x^*)}\frac{\partial \hat{\theta}}{\partial k(x)} \tag{A.19}$$

This equation characterizes the total effect of $k(x)$ on x^*, and completes the proof. □

Corollary 1

Proof. The total effect of $k(x)$ on x^* is given by:

$$\frac{\partial x^*}{\partial k(x)} = -\frac{\psi(pf)h\phi_{x\theta}(x^*, \hat{\theta})}{\psi(pf)h\phi_{xx}(x^*, \hat{\theta}) + c''(x^*)}\frac{\partial \hat{\theta}}{\partial k(x)} \tag{A.20}$$

By design, $\phi_{xx}(x^*, \hat{\theta}) > 0$ and $c''(x^*) > 0$, which implies that the sign of the relationship between $k(x)$ and x^* is completely characterized by the inverse of the product between $\phi_{x\theta}(x^*, \hat{\theta})$ and $\partial\hat{\theta}/\partial k(x)$. This statement completes the proof. □

B Supporting materials for regression analysis

In this section, we provide supporting material for the regression analyses in the study. Specifically, we provide the summary and regression tables not presented in the main text.

Tables B.1, B.2, and B.3 present the summary statistics for the pixel, voyage and IV analyses. They reveal notable regional differences in shipping traffic and piracy encounters. The Gulf of Aden and Southeast Asia are hotspots with significantly higher traffic, with average daily vessel occupancy at 38.2 and 78.1 hours per pixel, respectively, compared to 35.1 hours globally and only 11.9 hours in the Gulf of Guinea. Voyage-level data show vessels in hotspots travel longer distances and for more time, with the Gulf of Guinea experiencing the highest mean piracy encounters in the preceding three months. EEZ-based analysis highlights that the Gulf of Aden sees the most transit in terms of distance and time, despite the Gulf of Guinea having nearly double the number of piracy encounters, further underscoring the unique challenges faced by shippers in these regions.

Table B.1: Summary Statistics for Daily Ship Transit by Pixel.

	Distance (km)	Occupancy (hr)	Voyages (#)	Unique vessels (#)
Gulf of Aden				
Mean	708.6	38.2	14.3	14.1
SD	1,002.7	59.5	20.7	20.2
Median	126.4	9.4	3.0	3.0
Max	8,742.6	1,038.4	157.0	146.0
Gulf of Guinea				
Mean	137.8	11.9	3.3	3.3
SD	154.5	20.0	3.4	3.4
Median	97.8	5.8	3.0	2.0
Max	2,110.1	407.6	37.0	37.0
Southeast Asia				
Mean	1,085.3	78.1	18.5	17.6
SD	2,369.4	178.3	41.2	39.9
Median	247.0	20.8	4.0	4.0
Max	30,165.2	4,156.4	407.0	399.0
Rest of the World				
Mean	391.1	35.1	11.4	10.8
SD	919.6	79.1	26.6	25.4
Median	106.2	7.6	3.0	3.0
Max	16,593.6	2,172.6	261.0	247.0

Table B.4 reports the first-stage results from our IV analysis (Table 3). Overall, the analysis provides support for the validity of the instrument in the first stage. Increases in political stability are correlated with a decrease in pirate encounters in a given EEZ. This result is robust to the inclusion of the Gulf of Guinea dummy, and it highlights the potential importance of a country's economic and institutional state when it comes to the proliferation of piracy.

The results for the linear average effect of piracy are stacked in Table B.6 for fuel, labor, and total operational costs in thousands of US dollars, respectively. Across all samples, the results show that path adjustments increase fuel cost the most. One additional encounter relates to

Table B.2: Summary Statistics for Individual Voyage Features.

	Distance (km)	Time (hr)	Speed (km/hr)	Encounters (#/3 mo)
Gulf of Aden				
Mean	1,753.3	94.6	18.7	0.5
SD	3,060.6	217.5	7.4	1.2
Min	0.2	0.0	0.0	0.0
Max	421,538.8	37,861.1	115.5	25.0
Gulf of Guinea				
Mean	3,014.9	149.6	20.1	4.6
SD	4,040.2	238.4	7.5	5.8
Min	0.1	0.0	0.0	0.0
Max	468,276.4	33,372.3	58.6	45.0
Southeast Asia				
Mean	1,130.7	65.5	17.7	1.9
SD	2,768.4	266.8	6.6	5.0
Min	0.1	0.0	0.0	0.0
Max	813,656.8	51,409.2	130.2	44.0
Rest of the World				
Mean	608.8	30.9	21.5	0.1
SD	1,506.3	102.0	8.3	0.6
Min	0.0	0.0	0.0	0.0
Max	464,388.8	53,031.0	1,060.9	27.0

Table B.3: Summary Statistics for Traffic and Piracy at the EEZ level.

	Political Stability	Encounters (#)	Vessels (#)	Distance (km/vessel)	Time (hr/vessel)
Gulf of Aden					
Mean	-1.0	2.6	3,857.6	1,446.6	76.0
SD	1.0	5.1	3,148.3	1,277.3	59.2
Min	-3.0	0.0	212.0	30.5	1.2
Max	0.8	36.0	9,958.0	4,547.0	190.1
Gulf of Guinea					
Mean	-0.4	5.8	1,896.7	1,045.5	65.3
SD	0.7	11.6	721.6	607.6	36.8
Min	-2.1	0.0	660.0	247.0	11.3
Max	0.6	67.0	3,736.0	2,248.5	144.7

Table B.4: Political Stability and Yearly Pirate Encounters.

	(1)	(2)	(3)	(4)
Political Stability	−3.72***	−3.73***		−5.07***
	(1.17)	(1.20)		(1.40)
Gulf of Guinea Dummy			3.12***	6.47***
			(0.54)	(0.93)
Year FE		X	X	X

* $p < 0.1$, ** $p < 0.05$, *** $p < 0.01$ The unit of observation is a country. The sample spans from 2013 to 2021. Every column is a different specification. Political Stability is the index reported by the World Bank as part of its World Development Indicators. Additional covariates include a dummy variable if a country belongs to the Gulf of Guinea and yearly dummies. Standard errors are clustered by gulf by year. Number of observations is 180.

hundreds or thousands of dollars in additional fuel spent. These estimates are consistent with path adjustments. The results also suggest that vessels passing through the Gulf of Aden face the biggest burden with an additional US$5 thousand per encounter, while those in the Southeast Asia face the least.

These adjustments are also meaningful in terms of labor cost. The effects of additional encounters are positive and significant, but at most half of the adjustment cost when compared to additional fuel consumption. We note that this result is consistent across samples.

We estimate the effect of piracy on total operational costs by aggregating both fuel and labor costs. These results are reported in Panel (C) of Table B.6, and suggest that the average increase in operational costs due to avoidance measures per additional encounter ranges from over US$600 in the Gulf of Guinea to over US$6.4 thousand in the Gulf of Aden. Globally, this effect averages down to about US$800 for each additional pirate encounter.

The linear average effects of piracy on emissions are stacked in Table B.7 for CO_2, NO_x, and SO_x, respectively. As expected from previous results, excessive fuel consumption leads to excessive emissions across the spectrum of relevant pollutants. In particular, increases in CO_2 range from 2.6 to 35.15 tons per voyage per past pirate encounter. NO_x and SO_x emissions due to piracy are relatively less voluminous, though this is a direct consequence of their significantly smaller concentrations in bunker fuel relative to carbon. Nonetheless, regression estimates point to dozens of kilograms, and hundreds in the case of the Gulf of Aden, of excess pollutants emitted due to the presence of pirates.

Table B.5: Effect of Past Pirate Encounters on Shipping Cost.

	Global	G. of Aden	G. of Guinea	S.E. Asia
Panel (A): Fuel Cost (TUSD)				
Encounters (3 mo)	0.58***	5.12***	0.41***	0.49***
	(0.08)	(0.58)	(0.06)	(0.12)
Panel (B): Labor Cost (TUSD)				
Encounters (3 mo)	0.26***	1.31***	0.25***	0.23***
	(0.03)	(0.12)	(0.02)	(0.04)
Panel (C): Total Cost (TUSD)				
Encounters (3 mo)	0.83***	6.43***	0.66***	0.72***
	(0.11)	(0.66)	(0.07)	(0.14)
Observations	25,628,927	1,034,194	276,183	6,334,875
Hotspot FE	X	•	•	•

* $p < 0.1$, ** $p < 0.05$, *** $p < 0.01$ The unit of observation is a voyage. Each panel examines a calculated cost in terms of fuel cost, labor cost, and total cost as the sum of both. All coefficients are in thousands of US$. The sample spans from 2013 to 2021. Every column is a different sample: Global is the analysis using the whole sample. G. of Aden, S.E. Asia, and G. of Guinea restrict the sample to vessels passing through one of the hotspots, respectively. Every panel-column combination is a different regression analysis. Encounters (3mo) is the count of pirate encounters recorded in the projected path of the vessel in the preceding 90 days from the departure date using a 5 degree spatial footprint. Controls include average wind speed along the voyage and the wind-resistance index. Fixed effects include country-to-country combination, vessel type, vessel size, hotspot, and a battery of month by year and top port-to-port combination for country-to-country combination dummies.

Table B.6: Effect of Past Pirate Encounters on Shipping Cost.

	Global	G. of Aden	G. of Guinea	S.E. Asia
Panel (A): Fuel Cost (TUSD)				
Encounters (3 mo)	0.58***	5.12***	0.41***	0.49***
	(0.08)	(0.58)	(0.06)	(0.12)
Panel (B): Labor Cost (TUSD)				
Encounters (3 mo)	0.26***	1.31***	0.25***	0.23***
	(0.03)	(0.12)	(0.02)	(0.04)
Panel (C): Total Cost (TUSD)				
Encounters (3 mo)	0.83***	6.43***	0.66***	0.72***
	(0.11)	(0.66)	(0.07)	(0.14)
Observations	25,628,927	1,034,194	276,183	6,334,875
Hotspot FE	X	•	•	•

* $p < 0.1$, ** $p < 0.05$, *** $p < 0.01$ The unit of observation is a voyage. Each panel examines a calculated cost in terms of fuel cost, labor cost, and total cost as the sum of both. All coefficients are in thousands of US$. The sample spans from 2013 to 2021. Every column is a different sample: Global is the analysis using the whole sample. G. of Aden, S.E. Asia, and G. of Guinea restrict the sample to vessels passing through one of the hotspots, respectively. Every panel-column combination is a different regression analysis. Encounters (3mo) is the count of pirate encounters recorded in the projected path of the vessel in the preceding 90 days from the departure date using a 5 degree spatial footprint. Controls include average wind speed along the voyage and the wind-resistance index. Fixed effects include country-to-country combination, vessel type, vessel size, hotspot, and a battery of month by year and top port-to-port combination for country-to-country combination dummies.

Table B.7: Effect of Past Pirate Encounters on Shipping Emissions.

	Global	G. of Aden	G. of Guinea	S.E. Asia
Panel (A): CO_2 (tons)				
Encounters (3 mo)	3.50***	35.15***	4.29***	2.60***
	(0.37)	(3.85)	(0.39)	(0.36)
Panel (B): NO_x (kg)				
Encounters (3 mo)	85.70***	895.31***	106.15***	62.67***
	(9.29)	(99.26)	(10.00)	(8.96)
Panel (C): SO_x (kg)				
Encounters (3 mo)	72.95***	731.85***	89.29***	54.23***
	(7.79)	(80.07)	(8.17)	(7.55)
Observations	25,629,585	1,034,211	276,220	6,335,025
Hotspot FE	X	•	•	•

* $p < 0.1$, ** $p < 0.05$, *** $p < 0.01$ The unit of observation is a voyage. Each panel examines a calculated emission in terms of $textCO_2$ (tons), NO_x (kg), and SO_x (kg). The sample spans from 2013 to 2021. Every column is a different sample: Global is the analysis using the whole sample. G. of Aden, S.E. Asia, and G. of Guinea restrict the sample to vessels passing through one of the hotspots, respectively. Every panel-column combination is a different regression analysis. Encounters (3mo) is the count of pirate encounters recorded in the projected path of the vessel in the preceding 90 days from the departure date using a 5 degree spatial footprint. Controls include average wind speed along the voyage and the wind-resistance index. Fixed effects include country-to-country combination, vessel type, vessel size, hotspot, and a battery of month by year and top port-to-port combination for country-to-country combination dummies.

C Counterfactual costs and emissions

We use the fully specified *global* model (5° grid, 3 month window) to predict voyage-level fuel and labor costs, as well as emissions of CO_2, NO_x, and SO_x. We make predictions using the observed number of pirate encounters and a counterfactual of no pirate encounters at all. We then take the difference between these two predictions to obtain a voyage-level estimate of the additional fuel and labor costs, and emissions of each pollutant. We then calculate the total annual costs and emissions across all voyages. These results are shown in Table C.8 and Table C.9, where we also provide information disaggregated by hotspot.

Table C.8: Total Costs of Piracy to the Shipping Industry.

	2013	2014	2015	2016	2017	2018	2019	2020	2021
Fuel (Million USD)									
Global	1,099	1,274	1,571	988	1,036	553	478	1,325	1,210
G. of Aden	50	34	18	42	66	17	23	42	38
G. of Guinea	108	75	52	91	82	106	51	114	72
Southeast Asia	838	1,129	1,431	619	663	319	327	1,032	914
Labor (Million USD)									
Global	491	569	702	442	463	247	214	592	541
G. of Aden	22	15	8	19	29	7	10	19	17
G. of Guinea	48	34	23	41	37	47	23	51	32
Southeast Asia	374	505	640	277	297	142	146	461	409
Total (Million USD)									
Global	1,590	1,843	2,273	1,430	1,499	801	692	1,917	1,751
G. of Aden	72	49	26	61	95	24	33	61	55
G. of Guinea	156	109	75	131	119	153	74	164	104
Southeast Asia	1,212	1,634	2,072	896	960	461	473	1,493	1,323

Having matched each voyage to its additional costs and emissions, we then divide a voyage's cost (or emissions) across all 0.5°×0.5° pixels along which the vessel transited. For each pixel, we calculate the total surplus costs (fuel + labor) or emissions of each pollutant. We then take the average across all years (2013-2021) and use these data to produce maps shown in Figure 4A.

We are also interested in estimating the total public and private costs of modern-day piracy. We monetize the environmental impacts caused by additional emission of local and global air pollutants using their social-cost. Specifically, we use estimates provided by the Interagency Working Group on Social Cost of Greenhouse Gases (Interagency Working Group on Social Cost of Greenhouse Gases [United States Government], 2021), which suggest that an additional ton of CO_2 or NO_x induce damages valued at US\$51 and US\$18,000 (in 2020 US\$ assuming a 3% discount rate). For SO_x we use estimates from Mier, Adelowo, and Weissbart (Mier et al., 2021), which indicates an additional ton of SO2 inducing damages of US\$14,694 (in 2020 US\$). We then aggregate all information by ASAM region, and produce bar charts shown in Figure 4B.

Table C.9: Total Emission of Air Pollutants due to Piracy

	2013	2014	2015	2016	2017	2018	2019	2020	2021
CO_2 (Thousand metric tons)									
Global	5,325	6,226	7,622	4,740	5,144	2,727	2,356	6,479	5,968
G. of Aden	239	159	91	204	310	80	114	201	182
G. of Guinea	528	369	257	449	408	511	248	547	344
Southeast Asia	4,040	5,508	6,919	2,994	3,262	1,548	1,597	5,055	4,456
NOx (Metric tons)									
Global	130,242	152,280	186,422	115,938	125,818	66,712	57,625	158,464	145,986
G. of Aden	5,840	3,883	2,223	4,985	7,581	1,962	2,796	4,926	4,446
G. of Guinea	12,919	9,036	6,295	10,974	9,983	12,502	6,062	13,379	8,412
Southeast Asia	98,808	134,736	169,240	73,237	79,781	37,861	39,073	123,644	108,991
SOx (Metric tons)									
Global	110,861	129,620	158,682	98,686	107,096	56,786	49,051	134,885	124,263
G. of Aden	4,971	3,305	1,892	4,243	6,453	1,670	2,380	4,193	3,784
G. of Guinea	10,996	7,691	5,359	9,341	8,497	10,642	5,160	11,388	7,161
Southeast Asia	84,105	114,687	144,057	62,339	67,909	32,227	33,258	105,245	92,773

D Robustness tests

Here, we show robustness checks for all of the empirical results: how pirate encounters affect total shipping traffic within spatial grids, and how pirate encounters affect the features of individual voyages. The two sets of robustness checks largely follow the same pattern. Pirate encounters reduce traffic within pixels. These adjustments result in adjustments at the individual voyage level, which is then demonstrated by increase in the average total distance time traveled for the same port-to-port combination.

D.1 Pixel-level analysis

Here, we show evidence of the robustness of the pixel-level analysis. First, we show robustness to different sets of fixed effects in tabular form. The first set of results uses a global sample (Table D.10). Then, we repeat the exercise for the subset of pixels belonging to each of the three hotspots. The results for the Gulf of Aden, Gulf of Guinea, and Southeast Asia are presented in Table D.11, Table D.12, and Table D.13, respectively. In all tables, the fourth column presents the same results as Table 1 in the main text, which are the preferred specification including fixed-effects for pixel id, for ASAM subregion, and for ASAM region by year by month. All estimates from models with at least one fixed effect are relatively stable, with estimates always showing the same direction and similar magnitude as the preferred specification.

Second, we show robustness to using the total number of encounters occurring in a pixel over the last 3, 6 and 12 months. We find consistent evidence that additional past pirate encounters result in reduced vessel activity globally and across all three hotspots (Figure D.1). Additionally, lengthening the time window for encounters reduces the coefficient estimates because encounters far into the past are not as important as recent events.

Finally, as stated in our Methods, we also estimate dynamic effects in an event-study framework. Here, we use distance traveled (km), normalized distance traveled (km/vessel and km/voyage), occupancy time (hr), and normalized occupancy time (hr/vessel and hr/voyage) as our response variables. This analysis restricts the sample to pixels with no overlapping attacks five days before or after a given attack date (N = 233). The main results are shown in Figure D.2. As before we also test for different fixed-effect specifications (Figure D.3) and effects by hotspot (Figure D.4). The results are generally consistent and show a decrease in pixel-level activity following, but not leading to, an encounter.

Table D.10: Effect of Piracy on Pixel-level Ship Transit For Different Fixed-effects Specifications for a Global Sample.

	(1)	(2)	(3)	(4)
Panel (A): Total Distance (km)				
Encounters (3 mo)	484.96*	-14.76	-14.76	-4.90
	(284.26)	(12.53)	(12.53)	(11.53)
Panel (B): Occupancy (hr)				
Encounters (3 mo)	58.73*	7.75	7.75	8.42
	(31.50)	(6.86)	(6.86)	(6.73)
Panel (C): Voyages (#)				
Encounters (3 mo)	10.05*	-0.06	-0.06	0.32
	(5.94)	(0.47)	(0.47)	(0.44)
Panel (D): Vessels (#)				
Encounters (3 mo)	9.83*	-0.03	-0.03	0.35
	(5.85)	(0.48)	(0.48)	(0.45)
Pixel ID FE		X	X	X
ASAM Subregion FE			X	X
ASAM Region-year-month FE				X

* $p < 0.1$, ** $p < 0.05$, *** $p < 0.01$ The unit of observation is a pixel (N = 590 unique cells). The sample spans from 2013 to 2021. Each panel examines a measure of pixel-level ship transit in terms of total distance in kilometers (km), total occupancy time in hours (hr), and the number of unique voyages or vessels transiting through the pixel. Each column is a different regression analysis adding fixed-effects by pixel ID, then group, and finally time. Every panel-column combination is a different regression analysis. Encounters (3mo) is the count of pirate encounters recorded within the pixel in the preceding 90 days. Numbers in parentheses are Conley Standard Errors (100 km cutoff). Number of observations: 1,939,330.

Table D.11: Effect of Piracy on Pixel-level Ship Transit For Different Fixed-effects Specifications for the Gulf of Aden.

	(1)	(2)	(3)	(4)
Panel (A): Total Distance (km)				
Encounters (3 mo)	58.07	-30.57**	-30.57**	-26.50*
	(105.55)	(14.67)	(14.67)	(13.78)
Panel (B): Occupancy (hr)				
Encounters (3 mo)	7.91**	-0.89	-0.89	-0.70
	(3.84)	(1.05)	(1.05)	(1.20)
Panel (C): Voyages (#)				
Encounters (3 mo)	0.61	-1.05**	-1.05**	-0.67**
	(1.24)	(0.45)	(0.45)	(0.34)
Panel (D): Vessels (#)				
Encounters (3 mo)	0.62	-1.04**	-1.04**	-0.65*
	(1.24)	(0.44)	(0.44)	(0.34)
Pixel ID FE		X	X	X
ASAM Subregion FE			X	X
ASAM Region-year-month FE				X

* $p < 0.1$, ** $p < 0.05$, *** $p < 0.01$ The unit of observation is a pixel (N = 93 unique cells). The sample spans from 2013 to 2021. Each panel examines a measure of pixel-level ship transit in terms of total distance in kilometers (km), total occupancy time in hours (hr), and the number of unique voyages or vessels transiting through the pixel. Each column is a different regression analysis adding fixed-effects by pixel ID, then group, and finally time. Encounters (3mo) is the count of pirate encounters recorded within the pixel in the preceding 90 days. Numbers in parentheses are Conley Standard Errors (100 km cutoff). Number of observations: 305,691.

Table D.12: Effect of Piracy on Pixel-level Ship Transit For Different Fixed-effects Specifications for the Gulf of Guinea.

	(1)	(2)	(3)	(4)
Panel (A): Total Distance (km)				
Encounters (3 mo)	28.59	-4.80***	-4.80***	-4.58***
	(23.12)	(1.64)	(1.64)	(1.32)
Panel (B): Occupancy (hr)				
Encounters (3 mo)	6.84	-0.33	-0.33	-0.26
	(4.69)	(0.63)	(0.63)	(0.62)
Panel (C): Voyages (#)				
Encounters (3 mo)	0.94	-0.10***	-0.10***	-0.11***
	(0.64)	(0.03)	(0.03)	(0.04)
Panel (D): Vessels (#)				
Encounters (3 mo)	0.91	-0.10***	-0.10***	-0.10***
	(0.63)	(0.03)	(0.03)	(0.04)
Pixel ID FE		X	X	X
ASAM Subregion FE			X	X
ASAM Region-year-month FE				X

* $p < 0.1$, ** $p < 0.05$, *** $p < 0.01$ The unit of observation is a pixel (N = 134 unique cells). The sample spans from 2013 to 2021. Each panel examines a measure of pixel-level ship transit in terms of total distance in kilometers (km), total occupancy time in hours (hr), and the number of unique voyages or vessels transiting through the pixel. Each column is a different regression analysis adding fixed-effects by pixel ID, then group, and finally time. Encounters (3mo) is the count of pirate encounters recorded within the pixel in the preceding 90 days. Numbers in parentheses are Conley Standard Errors (100 km cutoff). Number of observations: 440,458.

Table D.13: Effect of Piracy on Pixel-level Ship Transit For Different Fixed-effects Specifications for Southeast Asia.

	(1)	(2)	(3)	(4)
Panel (A): Total Distance (km)				
Encounters (3 mo)	773.99***	-21.09	-21.09	-3.69
	(266.27)	(21.06)	(21.06)	(21.18)
Panel (B): Occupancy (hr)				
Encounters (3 mo)	91.82***	14.70	14.70	15.97
	(34.42)	(10.35)	(10.35)	(9.89)
Panel (C): Voyages (#)				
Encounters (3 mo)	16.56***	0.14	0.14	0.79
	(5.87)	(0.79)	(0.79)	(0.68)
Panel (D): Vessels (#)				
Encounters (3 mo)	16.22***	0.21	0.21	0.83
	(5.79)	(0.80)	(0.80)	(0.69)
Pixel ID FE		X	X	X
ASAM Subregion FE			X	X
ASAM Region-year-month FE				X

* $p < 0.1$, ** $p < 0.05$, *** $p < 0.01$ The unit of observation is a pixel (N = 149 unique cells). The sample spans from 2013 to 2021. Each panel examines a measure of pixel-level ship transit in terms of total distance in kilometers (km), total occupancy time in hours (hr), and the number of unique voyages or vessels transiting through the pixel. Each column is a different regression analysis adding fixed-effects by pixel ID, then group, and finally time. Encounters (3mo) is the count of pirate encounters recorded within the pixel in the preceding 90 days. Numbers in parentheses are Conley Standard Errors (100 km cutoff). Number of observations: 489,763.

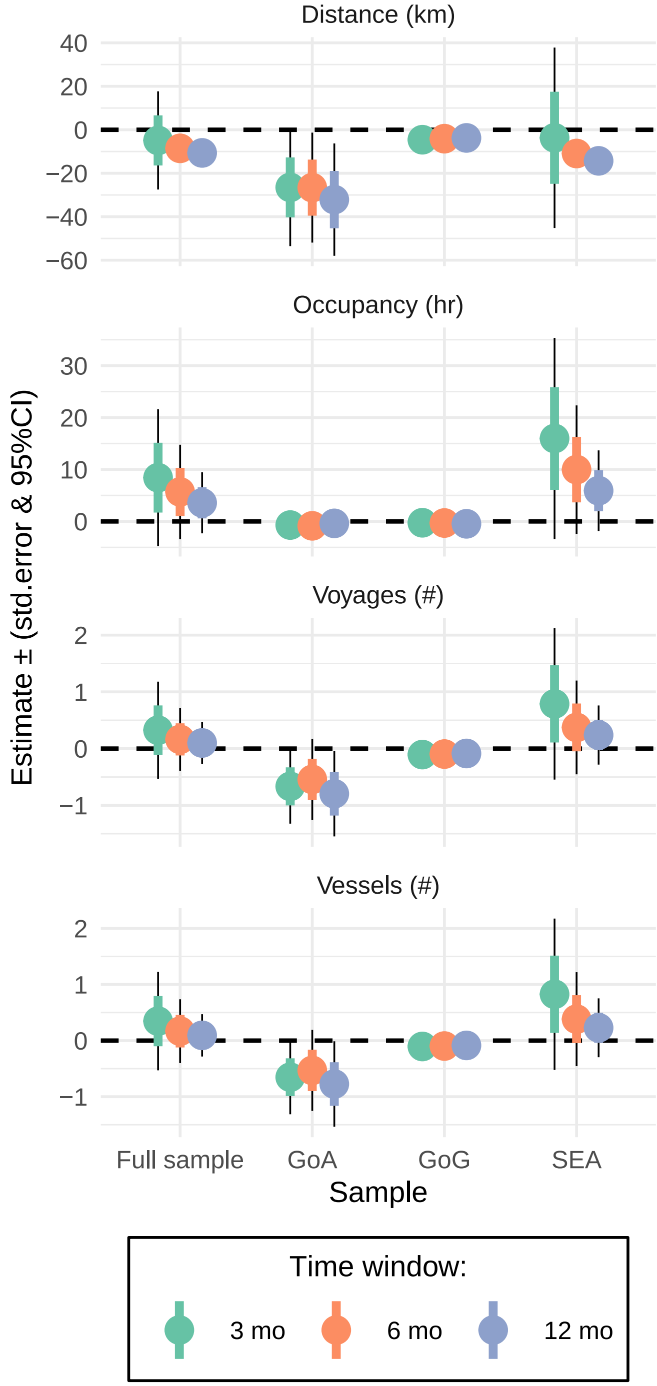

Figure D.1: **Average piracy effect on pixel-level ship transit.** The x-axis shows the sub-sample and the y-axis the estimated effect. Each marker indicates a coefficient estimate for the average effect of the number of attacks over the last 3, 6, or 12 months on the measure of ship transit shown in each panel. The colored portion of error bars show standard errors and the black portion of the error bars shows 95% CIs. Note how increasing the time window results in attenuated coefficients.

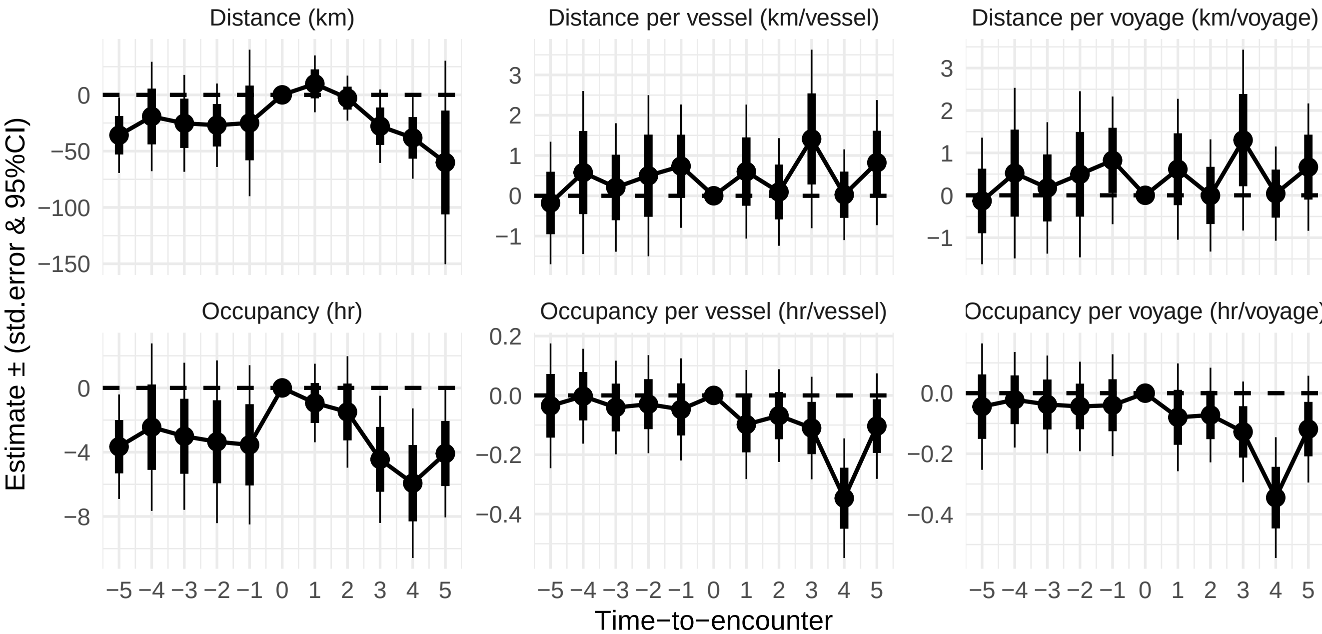

Figure D.2: **Event-study for the effect of piracy attacks on ship transit.** The top row shows coefficient estimates with distance (km) and normalized distance (km/vessel and km/voyage) as the dependent variable. The bottom row uses occupancy time (hours) and normalized occupancy time (hr/vessel and hr/voyage) as the dependent variable. We estimate a total of 10 coefficients and our sample contains 233 pixels. Coefficients show the change in transit relative to the day of attack (i.e., Time-to-encounter = 0). The thick portion of error bars are spatial Conley standard errors using a 100 km radius and the thin portion of error bars shows 95%CIs. All estimations include fixed effects by ASAM subregion, Year-by-month-by-ASAM region, and pixel-id.

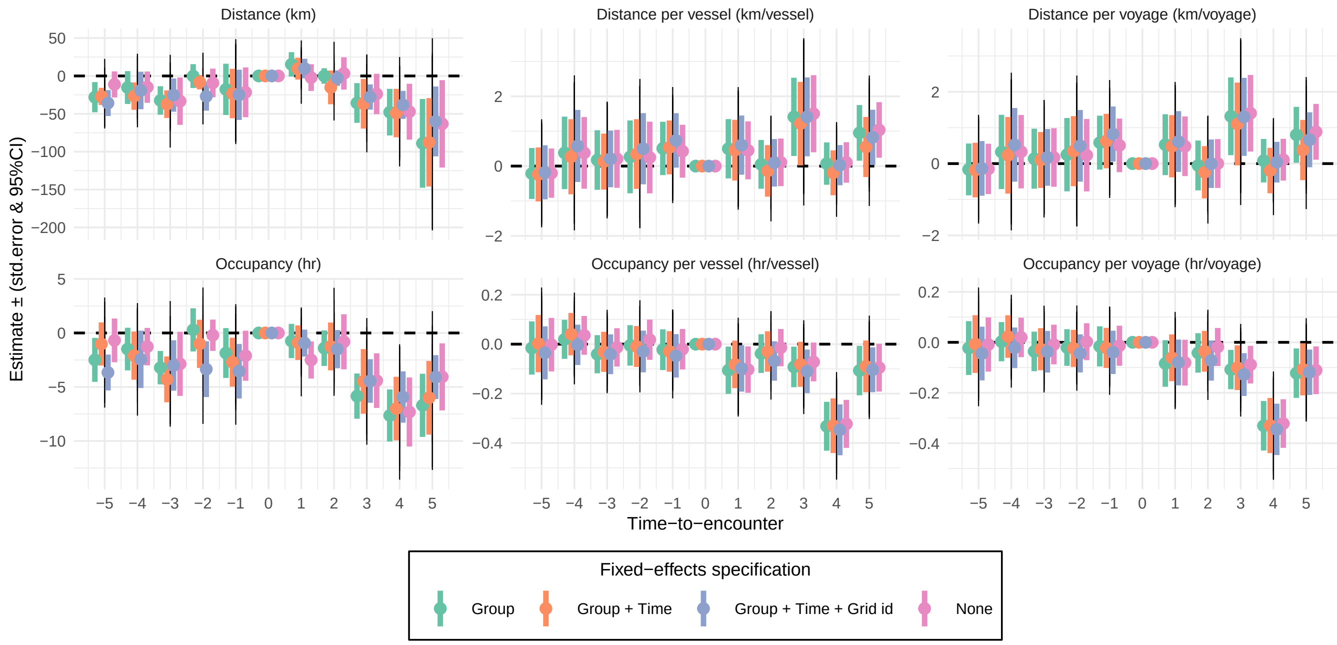

Figure D.3: **Build-up to a Two-way fixed effects specification.** The top row shows coefficient estimates with distance (km) and normalized distance (km/vessel and km/voyage) as the dependent variable. The bottom row uses occupancy time (hours) and normalized occupancy time (hr/vessel and hr/voyage) as the dependent variable. We estimate a total of 10 coefficients and our sample contains 233 pixels. Coefficients show the change in transit relative to the day of attack (i.e., Time-to-encounter = 0). Colors indicate different fixed-effects specification. The thick portion of error bars are spatial Conley standard errors using a 100 km radius and the thin portion of error bars shows 95%CIs.The preferred specification contains fixed-effects for group, time, and observational unit and are equivalent to these shown in Figure D.2.

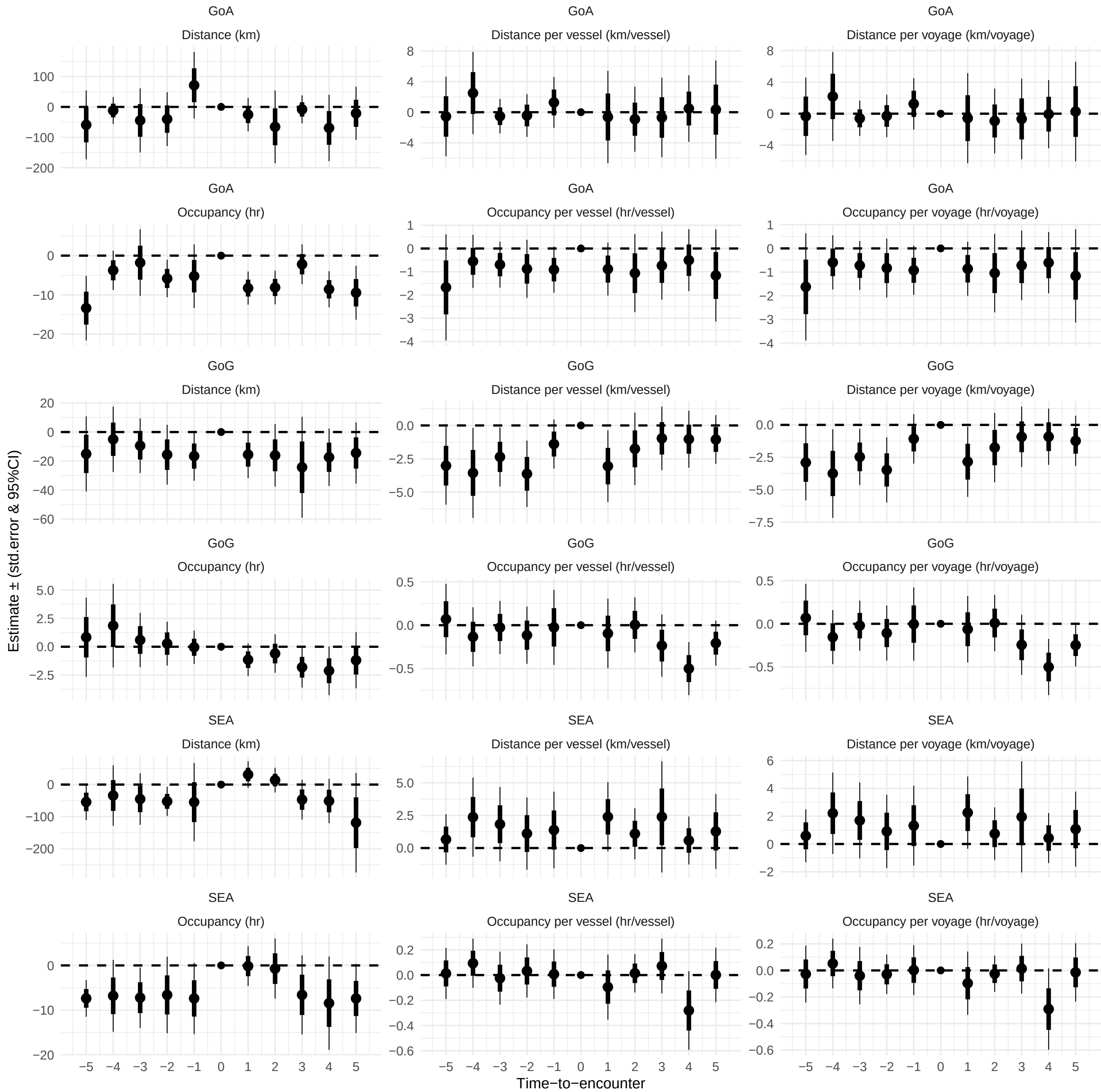

Figure D.4: **Event-study for the effect of piracy attacks on ship transit by hotspot.** Each row shows a combination of hotspot - measure. We estimate a total of 10 coefficients, which show the change in transit relative to the day of attack (i.e., Time-to-encounter = 0). The thick portion of error bars are spatial Conley standard errors using a 100 km radius and the thin portion of error bars shows 95%CIs. All estimations include fixed effects by ASAM subregion, Year-by-month-by-ASAM region, and pixel-id.

D.2 Voyage-level analysis

Here we present evidence of the robustness of the voyage analysis to several modeling assumptions. First, we show robustness to different sets of fixed effects in tabular form. The estimates are sensitive to the inclusion of country-to-country fixed effects, but this is expected as the length and specific paths of each route are bound to vary widely across combinations. The suite of results are included in Tables D.14 to D.22. Overall, the results are highly robust to the addition of vessel, hotspot and top route fixed effects. The results are also robust to the inclusion of weather controls in the form of wind speed and wind-resistance index.

Second, we show robustness to i) using a rolling window of 3, 6, and 12 months, as well as the use of a global 3°x3°, 0.5°×0.5°, and 7°x7° grid to construct the past encounters variable. This approach allows us to test the temporal and spatial sensitivity of our analysis and the results are shown in Figure D.5. The results show that the effect of recent encounters diminishes when longer time windows are considered and that working with larger spatial footprints (i.e., 7°x7°) tends to attenuate results toward zero. For completeness, we will maintain these sensitivities in all of the analyses below.

Third, we show robustness of the results to the categorization of cargo vessels. In the main analysis, we use the best available vessel class for each individual vessel as categorized by Global Fishing Watch. This 'best available' approach uses the vessel class provided by official registries where available, and infers vessel class using a neural network when registries are not available (Kroodsma et al., 2018). As a robustness check, we restrict the analysis to work with: 1) vessels that are always categorized as cargo vessels according to official registries; as well as 2) expand it as those who are categorized in official registries as being cargo vessels at least once. These results are shown in Figure D.6 and Figure D.7 and are virtually unchanged with respect to the results in the main analysis, though minimal changes around zero are detected for the speed analysis. We reiterate that the magnitudes detected for speed are practically meaningless.

Fourth, we show robustness to the definition of our explanatory variable. For each voyage, we calculate the total number of unique encounters that occurred along all previously traveled paths (i.e., surrogate trips), as well as the chosen path, for each port-to-port route within the preceding months of a voyage's departure. This represents, for any given voyage departure date for any given port-to-port route, the captain's assessment of the prevalence of piracy along the universe of potential paths that have been recently traveled along the route. We call this variable "Total Number of Encounters." The results from this test are shown in Figure D.9 and are consistent with the main analysis, though there is considerable attenuation. This is expected, as the marginal impact of an additional pirate encounter diminishes as the potential area of paths along a route increases.

In addition, for each voyage we calculate the average number of unique attacks that occurred along all previously traveled paths (i.e., surrogate trips) for that port-to-port route within a time window. This represents, for any given voyage departure date for any given port-to-port route, the captain's expectation of how many attacks they might expect could occur along the route. We call this variable "Average Number of Encounters." This analysis is presented in Figure D.9, and shows considerable attenuation. Positive effects in terms of distance are detected, except in Southeast Asia. Effects in terms of time are mostly dissipated. This result is expected, as it is again easy to see the marginal impact of an additional pirate encounter diminishes further as its effect is now diluted by a considerably increase in the spatial footprint considered, over the number of voyages that took place before.

Finally, we show robustness of the results to the addition of speed and days since the last encounter along a route as *covariates*. The results are shown in Figure D.10, and are practically unchanged and provide support that the main adjustments are not polluted by not controlling for voyage speed or other short-term features of risk.

Table D.14: Effect of Past Pirate Encounters on Voyage Distance.

	(1)	(2)	(3)	(4)	(5)	(6)
Encounters (3 mo)	146.59***	134.88***	28.03***	27.17***	26.94***	26.92***
	(15.40)	(14.54)	(3.75)	(3.56)	(3.59)	(3.58)
Wind Speed (m/s)		305.58***	43.21***	42.03***	31.54***	31.29***
		(24.57)	(4.18)	(3.52)	(4.77)	(4.91)
Wind Resistance Index (m/s) (m/s)		97.15***	11.02***	−2.10**	−2.19**	−2.78***
		(7.85)	(1.47)	(0.90)	(0.94)	(0.90)
Observations	19,478,531	19,475,535	19,475,535	19,475,525	19,475,525	19,475,525
Country Combo. FE			X	X	X	X
Vessel Type FE				X	X	X
Vessel Size FE				X	X	X
Hotspot FE					X	X
Top Route FE						X
Month-by-Year FE	X	X	X	X	X	X

* $p < 0.1$, ** $p < 0.05$, *** $p < 0.01$ The unit of observation is a voyage. The sample spans from 2013 to 2021. Every column is a different specification. Encounters (3mo) is the count of pirate encounters recorded in the projected path of the vessel in the preceding 90 days from the departure date using a 5 degree spatial footprint. Fixed effects include country-to-country combination, vessel type, vessel size, hotspot, and a battery of month by year and top port-to-port combination for country-to-country combination dummies.

Table D.15: Effect of Past Pirate Encounters on Voyage Time.

	(1)	(2)	(3)	(4)	(5)	(6)
Encounters (3 mo)	7.60***	7.12***	2.29***	2.26***	2.25***	2.25***
	(0.65)	(0.62)	(0.33)	(0.33)	(0.33)	(0.33)
Wind Speed (m/s)		12.96***	1.94***	1.91***	1.15***	1.12***
		(0.99)	(0.23)	(0.21)	(0.33)	(0.34)
Wind Resistance Index (m/s)		3.72***	0.13**	−0.09*	−0.10*	−0.15***
		(0.36)	(0.05)	(0.05)	(0.05)	(0.05)
Observations	19,478,531	19,475,535	19,475,535	19,475,525	19,475,525	19,475,525
Country Combo. FE			X	X	X	X
Vessel Type FE				X	X	X
Vessel Size FE				X	X	X
Hotspot FE					X	X
Top Route FE						X
Month-by-Year FE	X	X	X	X	X	X

* $p < 0.1$, ** $p < 0.05$, *** $p < 0.01$ The unit of observation is a voyage. The sample spans from 2013 to 2021. Every column is a different specification. Encounters (3mo) is the count of pirate encounters recorded in the projected path of the vessel in the preceding 90 days from the departure date using a 5 degree spatial footprint. Fixed effects include country-to-country combination, vessel type, vessel size, hotspot, and a battery of month by year and top port-to-port combination for country-to-country combination dummies.

Table D.16: Effect of Past Pirate Encounters on Voyage Speed.

	(1)	(2)	(3)	(4)	(5)	(6)
Encounters (3 mo)	0.13***	0.11***	0.01*	−0.01*	−0.01*	−0.01*
	(0.02)	(0.02)	(0.01)	(0.01)	(0.01)	(0.01)
Wind Speed (m/s)		0.43***	0.09***	0.07***	0.06***	0.06***
		(0.05)	(0.02)	(0.01)	(0.01)	(0.01)
Wind Resistance Index (m/s)		0.55***	0.30***	0.01	0.01	0.01
		(0.03)	(0.02)	(0.01)	(0.01)	(0.01)
Observations	25,641,468	25,632,270	25,632,270	25,632,233	25,632,233	25,632,233
Country Combo. FE			X	X	X	X
Vessel Type FE				X	X	X
Vessel Size FE				X	X	X
Hotspot FE					X	X
Top Route FE						X
Month-by-Year FE	X	X	X	X	X	X

* $p < 0.1$, ** $p < 0.05$, *** $p < 0.01$ The unit of observation is a voyage. The sample spans from 2013 to 2021. Every column is a different specification. Encounters (3mo) is the count of pirate encounters recorded in the projected path of the vessel in the preceding 90 days from the departure date using a 5 degree spatial footprint. Fixed effects include country-to-country combination, vessel type, vessel size, hotspot, and a battery of month by year and top port-to-port combination for country-to-country combination dummies.

Table D.17: Effect of Past Pirate Encounters on Fuel Cost.

	(1)	(2)	(3)	(4)	(5)	(6)
Encounters (3 mo)	3.07***	2.83***	0.63***	0.58***	0.58***	0.58***
	(0.28)	(0.27)	(0.09)	(0.08)	(0.08)	(0.08)
Wind total (m/s)		6.25***	0.91***	0.80***	0.62***	0.62***
		(0.46)	(0.08)	(0.08)	(0.08)	(0.08)
Wind Resistance Index (m/s)		1.99***	0.28***	−0.08***	−0.09***	−0.09***
		(0.15)	(0.04)	(0.02)	(0.02)	(0.02)
Observations	25,638,777	25,629,585	25,629,585	25,629,585	25,629,585	25,629,585
Country Combo. FE			X	X	X	X
Vessel Type FE				X	X	X
Vessel Size FE				X	X	X
Hotspot FE					X	X
Top Route FE						X
Month-by-Year FE	X	X	X	X	X	X

* $p < 0.1$, ** $p < 0.05$, *** $p < 0.01$ The unit of observation is a voyage. The sample spans from 2013 to 2021. Every column is a different specification. Encounters (3mo) is the count of pirate encounters recorded in the projected path of the vessel in the preceding 90 days from the departure date using a 5 degree spatial footprint. Fixed effects include country-to-country combination, vessel type, vessel size, hotspot, and a battery of month by year and top port-to-port combination for country-to-country combination dummies.

Table D.18: Effect of Past Pirate Encounters on Labor Cost

	(1)	(2)	(3)	(4)	(5)	(6)
Encounters (3 mo)	0.99***	0.92***	0.27***	0.26***	0.26***	0.26***
	(0.09)	(0.08)	(0.04)	(0.03)	(0.03)	(0.03)
Wind total (m/s)		1.77***	0.28***	0.27***	0.20***	0.20***
		(0.13)	(0.03)	(0.02)	(0.03)	(0.03)
Wind Resistance Index (m/s)		0.61***	0.10***	0.00	0.00	−0.01
		(0.04)	(0.01)	(0.01)	(0.01)	(0.01)
Observations	25,638,777	25,629,585	25,629,585	25,629,585	25,629,585	25,629,585
Country Combo. FE			X	X	X	X
Vessel Type FE				X	X	X
Vessel Size FE				X	X	X
Hotspot FE					X	X
Top Route FE						X
Month-by-Year FE	X	X	X	X	X	X

* p < 0.1, ** p < 0.05, *** p < 0.01 The unit of observation is a voyage. The sample spans from 2013 to 2021. Every column is a different specification. Encounters (3mo) is the count of pirate encounters recorded in the projected path of the vessel in the preceding 90 days from the departure date using a 5 degree spatial footprint. Fixed effects include country-to-country combination, vessel type, vessel size, hotspot, and a battery of month by year and top port-to-port combination for country-to-country combination dummies.

Table D.19: Effect of Past Pirate Encounters on Total Cost.

	(1)	(2)	(3)	(4)	(5)	(6)
Encounters (3 mo)	4.06***	3.75***	0.89***	0.84***	0.83***	0.83***
	(0.36)	(0.34)	(0.11)	(0.11)	(0.11)	(0.11)
Wind total (m/s)		8.02***	1.18***	1.07***	0.82***	0.82***
		(0.59)	(0.11)	(0.10)	(0.10)	(0.11)
Wind Resistance Index (m/s)		2.60***	0.38***	−0.09***	−0.09***	−0.09***
		(0.19)	(0.05)	(0.02)	(0.02)	(0.02)
Observations	25,638,777	25,629,585	25,629,585	25,629,585	25,629,585	25,629,585
Country Combo. FE			X	X	X	X
Vessel Type FE				X	X	X
Vessel Size FE				X	X	X
Hotspot FE					X	X
Top Route FE						X
Month-by-Year FE	X	X	X	X	X	X

* p < 0.1, ** p < 0.05, *** p < 0.01 The unit of observation is a voyage. The sample spans from 2013 to 2021. Every column is a different specification. Encounters (3mo) is the count of pirate encounters recorded in the projected path of the vessel in the preceding 90 days from the departure date using a 5 degree spatial footprint. Fixed effects include country-to-country combination, vessel type, vessel size, hotspot, and a battery of month by year and top port-to-port combination for country-to-country combination dummies.

Table D.20: Effect of Past Pirate Encounters on CO_2 emissions

	(1)	(2)	(3)	(4)	(5)	(6)
Encounters (3 mo)	22.12***	20.39***	3.86***	3.55***	3.50***	3.50***
	(1.99)	(1.89)	(0.41)	(0.37)	(0.37)	(0.37)
Wind Speed (m/s)		45.78***	6.52***	5.72***	4.45***	4.46***
		(3.35)	(0.55)	(0.48)	(0.52)	(0.52)
Wind Resistance Index (m/s)		14.62***	2.16***	−0.54***	−0.56***	−0.55***
		(1.02)	(0.22)	(0.12)	(0.12)	(0.12)
Observations	25,638,777	25,629,585	25,629,585	25,629,585	25,629,585	25,629,585
Country Combo. FE			X	X	X	X
Vessel Type FE				X	X	X
Vessel Size FE				X	X	X
Hotspot FE					X	X
Top Route FE						X
Month-by-Year FE	X	X	X	X	X	X

* p < 0.1, ** p < 0.05, *** p < 0.01 The unit of observation is a voyage. The sample spans from 2013 to 2021. Every column is a different specification. Encounters (3mo) is the count of pirate encounters recorded in the projected path of the vessel in the preceding 90 days from the departure date using a 5 degree spatial footprint. Fixed effects include country-to-country combination, vessel type, vessel size, hotspot, and a battery of month by year and top port-to-port combination for country-to-country combination dummies.

Table D.21: Effect of Past Pirate Encounters on NO_x Emissions

	(1)	(2)	(3)	(4)	(5)	(6)
Encounters (3 mo)	557.07***	512.92***	94.62***	86.75***	85.69***	85.69***
	(50.38)	(47.69)	(10.08)	(9.27)	(9.28)	(9.29)
Wind total (m/s)		1,166.35***	164.94***	144.48***	112.84***	113.01***
		(85.33)	(14.01)	(12.34)	(13.10)	(13.05)
Wind Resistance Index (m/s)		370.58***	53.17***	−15.21***	−15.75***	−15.37***
		(25.88)	(5.80)	(3.25)	(3.28)	(3.28)
Observations	25,638,777	25,629,585	25,629,585	25,629,585	25,629,585	25,629,585
Country Combo. FE			X	X	X	X
Vessel Type FE				X	X	X
Vessel Size FE				X	X	X
Hotspot FE					X	X
Top Route FE						X
Month-by-Year FE	X	X	X	X	X	X

* p < 0.1, ** p < 0.05, *** p < 0.01 The unit of observation is a voyage. The sample spans from 2013 to 2021. Every column is a different specification. Encounters (3mo) is the count of pirate encounters recorded in the projected path of the vessel in the preceding 90 days from the departure date using a 5 degree spatial footprint. Fixed effects include country-to-country combination, vessel type, vessel size, hotspot, and a battery of month by year and top port-to-port combination for country-to-country combination dummies.

Table D.22: Effect of Past Pirate Encounters on SO_x Emissions.

	(1)	(2)	(3)	(4)	(5)	(6)
Encounters (3 mo)	460.59***	424.49***	80.34***	73.83***	72.94***	72.94***
	(41.47)	(39.27)	(8.47)	(7.77)	(7.78)	(7.79)
Wind total (m/s)		953.21***	135.73***	119.06***	92.71***	92.79***
		(69.77)	(11.50)	(10.07)	(10.81)	(10.79)
Wind Resistance Index (m/s)		304.32***	44.97***	−11.25***	−11.70***	−11.51***
		(21.26)	(4.62)	(2.49)	(2.52)	(2.52)
Observations	25,638,777	25,629,585	25,629,585	25,629,585	25,629,585	25,629,585
Country Combo. FE			X	X	X	X
Vessel Type FE				X	X	X
Vessel Size FE				X	X	X
Hotspot FE					X	X
Top Route FE						X
Month-by-Year FE	X	X	X	X	X	X

* $p < 0.1$, ** $p < 0.05$, *** $p < 0.01$ The unit of observation is a voyage. The sample spans from 2013 to 2021. Every column is a different specification. Encounters (3mo) is the count of pirate encounters recorded in the projected path of the vessel in the preceding 90 days from the departure date using a 5 degree spatial footprint. Fixed effects include country-to-country combination, vessel type, vessel size, hotspot, and a battery of month by year and top port-to-port combination for country-to-country combination dummies.

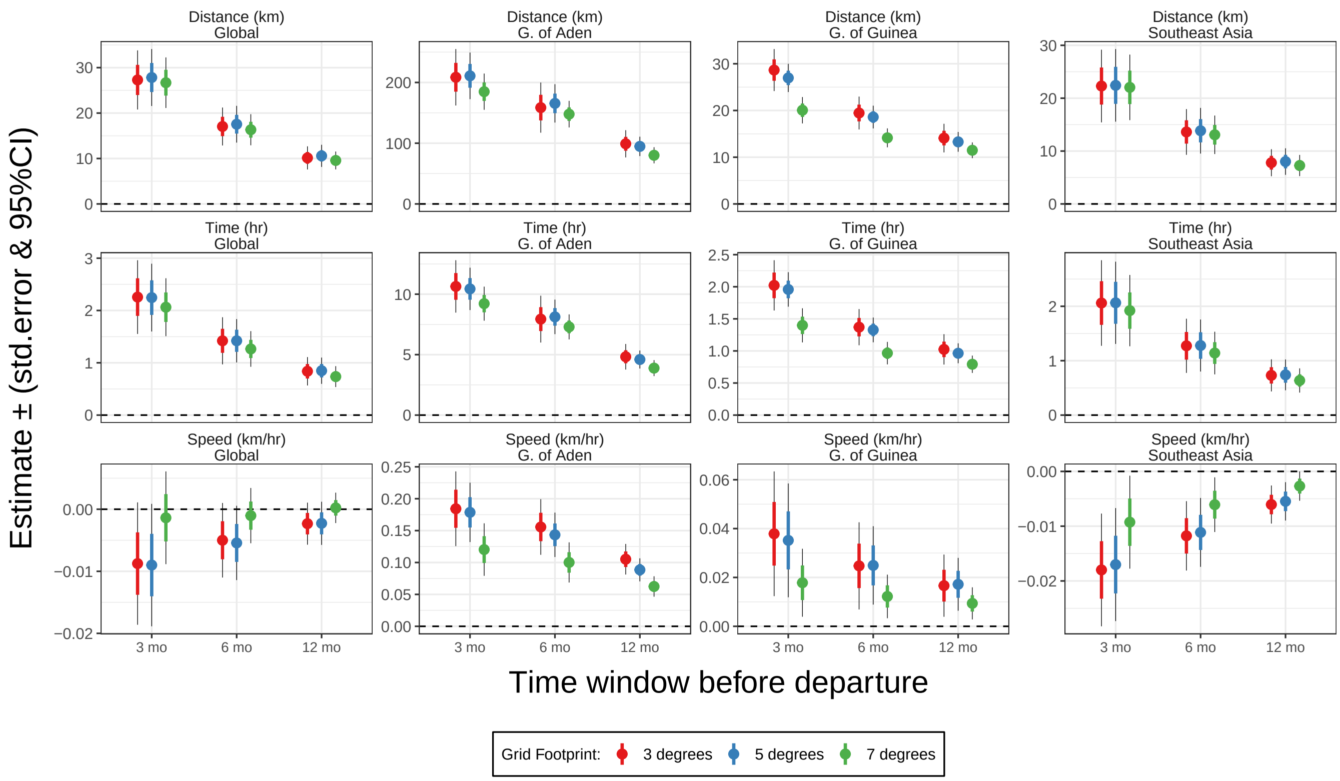

Figure D.5: **Replication Under Different Time Horizons and Degree Footprints.** Coefficients show the change in voyage features as a function of the number of pirate encounters in the preceding months. The analysis is conducted for all the variables and subsamples reported in the main text. Each plot shows the results for models using time windows of 3, 6, and, 12 months, respectively. Each color shows results for models using a 3, 5, and 7° spatial footprint, respectively. The thick portion of error bars are the clustered standard errors, and the thin portion of error bars shows 95%CIs. Estimation, subsampling, specification, and clustering approach remain identical to those in Table 2.

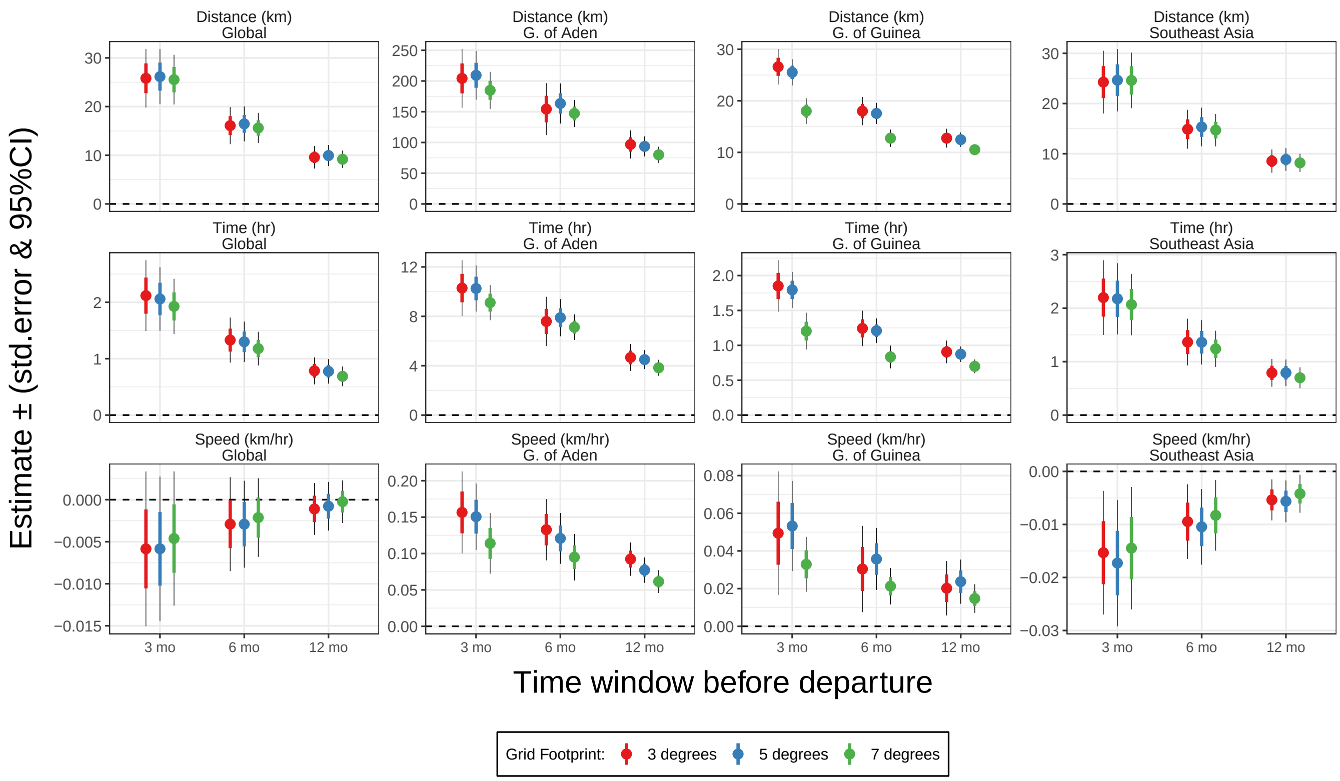

Figure D.6: **Replication Under Different Time Horizons and Degree Footprints of Vessels Always Classified as Cargo.** Coefficients show the change in voyage features as a function of the number of pirate encounters in the preceding months. The analysis is conducted for all the variables and subsamples reported in the main text. Each plot shows the results for models using time windows of 3, 6, and, 12 months, respectively. Each color shows results for models using a 3, 5, and 7° spatial footprint, respectively. The thick portion of error bars are the clustered standard errors, and the thin portion of error bars shows 95%CIs. Estimation, subsampling, specification, and clustering approach remain identical to those in Table 2.

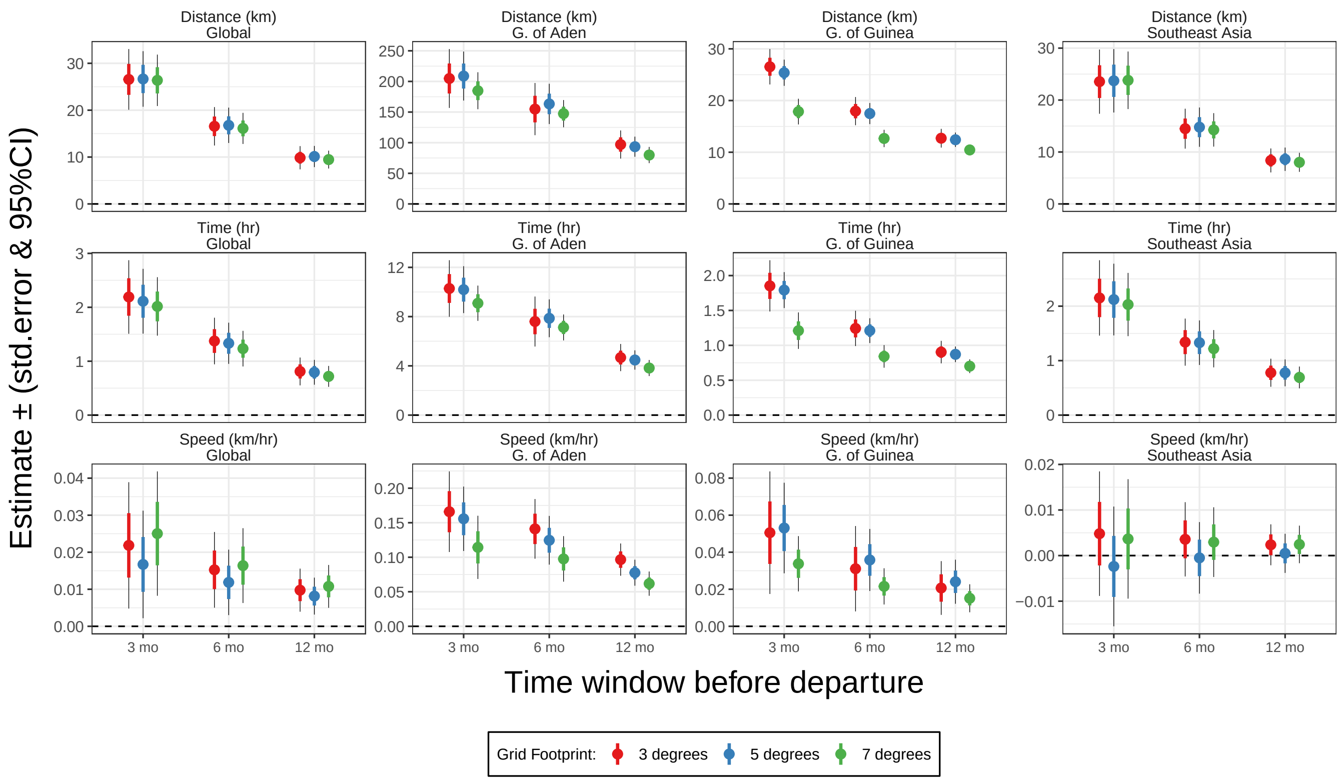

Figure D.7: **Replication Under Different Time Horizons and Degree Footprints of Vessels at Least Once Classified as Cargo.** Coefficients show the change in voyage features as a function of the number of pirate encounters in the preceding months. The analysis is conducted for all the variables and subsamples reported in the main text. Each plot shows the results for models using time windows of 3, 6, and, 12 months, respectively. Each color shows results for models using a 3, 5, and 7° spatial footprint, respectively. The thick portion of error bars are the clustered standard errors, and the thin portion of error bars shows 95%CIs. Estimation, subsampling, specification, and clustering approach remain identical to those in Table 2.

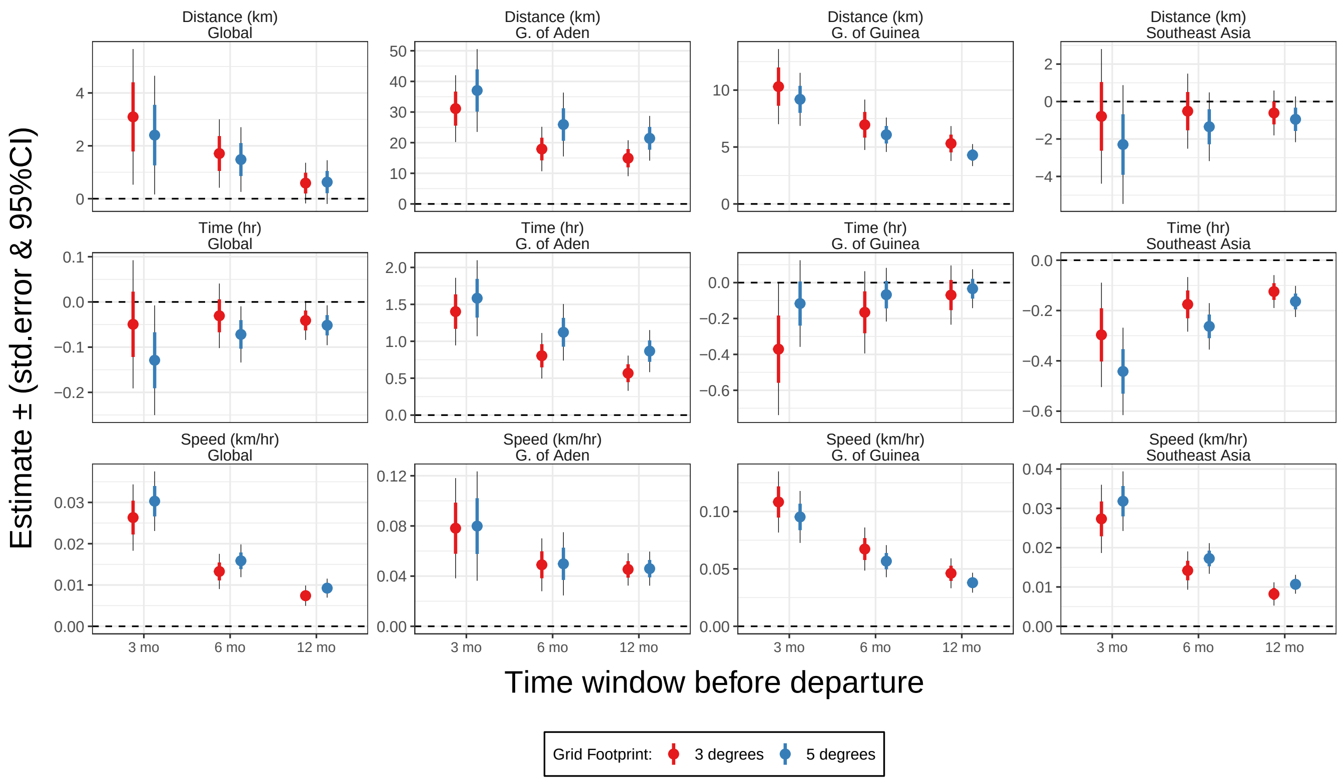

Figure D.8: **Replication Using Average Number of Encounters Under Different Time Horizons and Degree Footprints.** Coefficients show the change in voyage features as a function of the average number of pirate encounters experienced by other vessels in the preceding months. The analysis is conducted for all the variables and subsamples reported in the main text. Each plot shows the results for models using time windows of 3, 6, and, 12 months, respectively. Each color shows results for models using a 3 and 5° spatial footprint, respectively. The thick portion of error bars are the clustered standard errors, and the thin portion of error bars shows 95%CIs. Other than the explanatory variable, estimation, subsampling, specification, and clustering approach remain identical to those in Table 2.

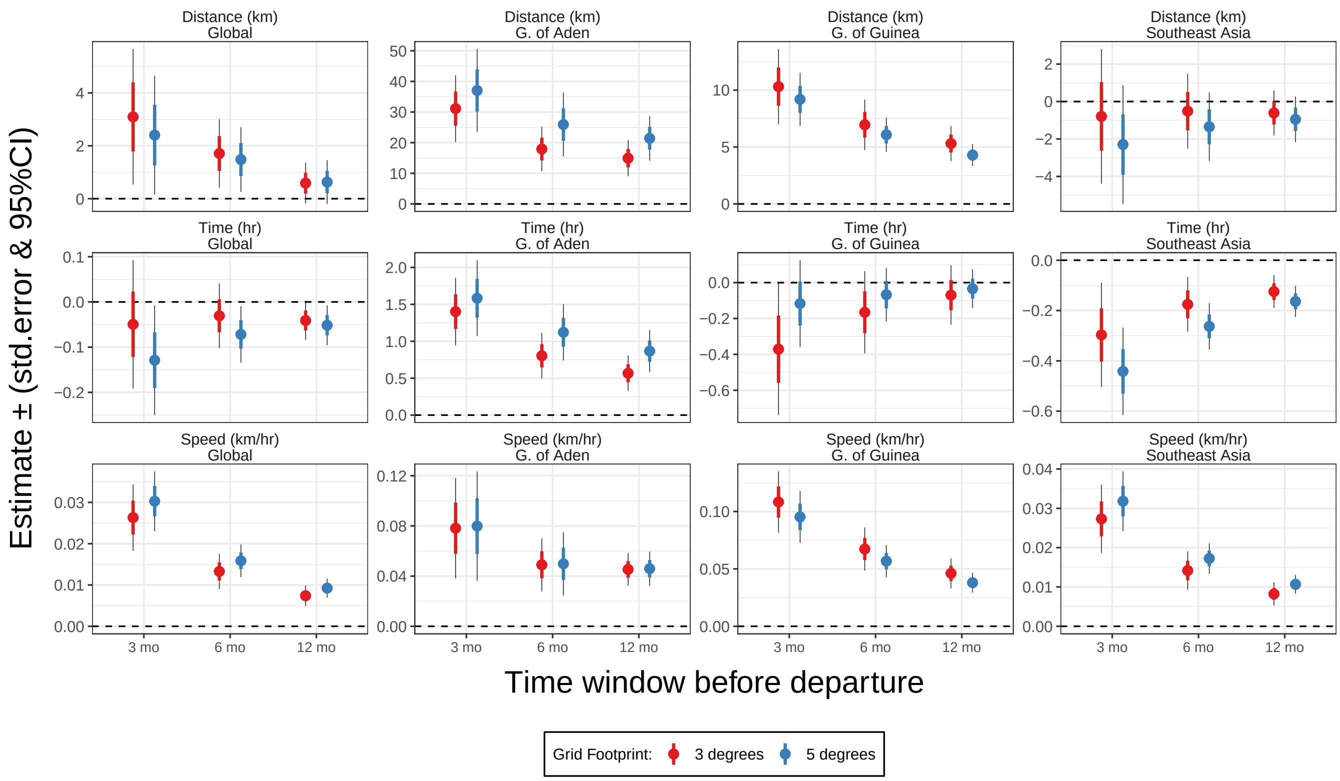

Figure D.9: **Replication Using Total Number of Encounters Under Different Time Horizons and Degree Footprints.** Coefficients show the change in voyage features as a function of the average number of pirate encounters experienced by other vessels in the preceding months. The analysis is conducted for all the variables and subsamples reported in the main text. Each plot shows the results for models using time windows of 3, 6, and, 12 months, respectively. Each color shows results for models using a 3 and 5° spatial footprint, respectively. The thick portion of error bars are the clustered standard errors, and the thin portion of error bars shows 95%CIs. Other than the explanatory variable, estimation, subsampling, specification, and clustering approach remain identical to those in Table 2.

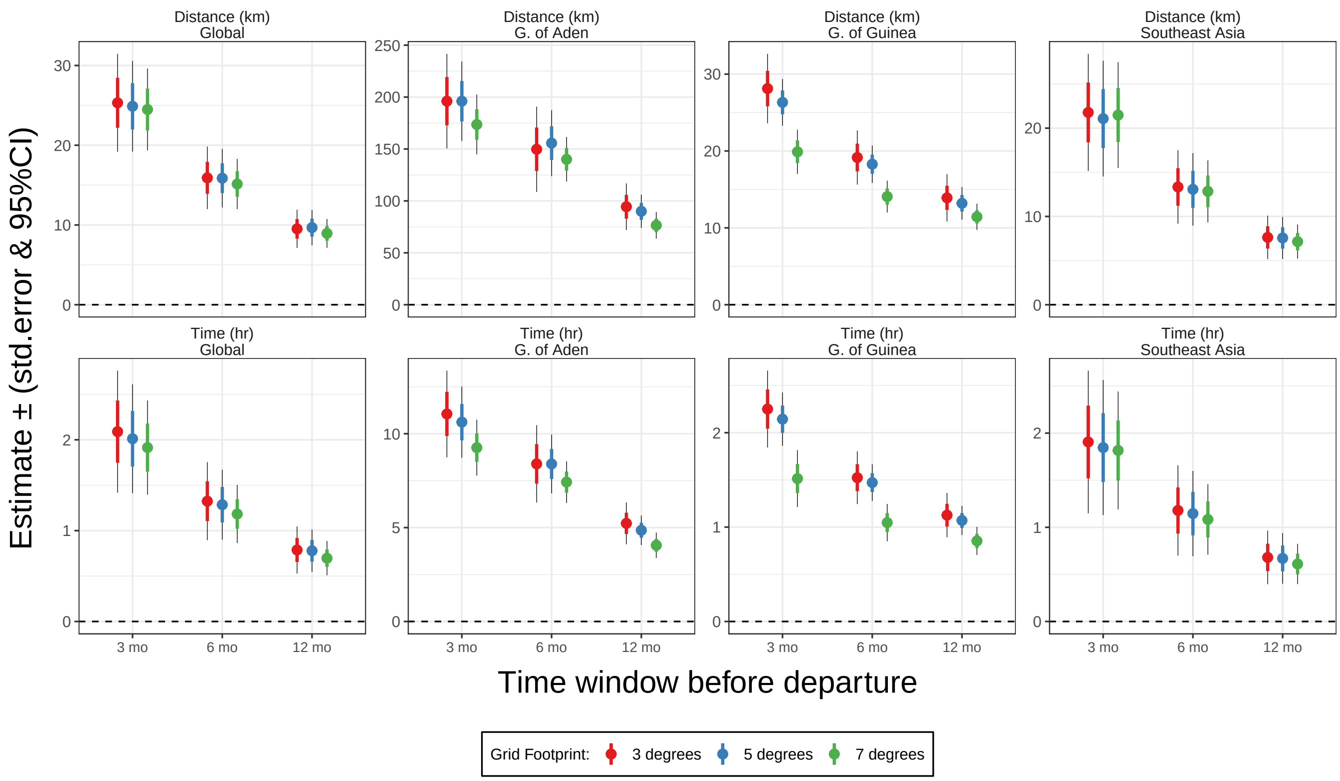

Figure D.10: **Replication Using Speed and Days Since Last Encounter as Covariates Under Different Time Horizons and Degree Footprints.** Coefficients show the change in voyage features as a function of the average number of pirate encounters experienced by other vessels in the preceding months. The analysis is conducted for all the variables and subsamples reported in the main text. Each plot shows the results for models using time windows of 3, 6, and, 12 months, respectively. Each color shows results for models using a 3 and 5° spatial footprint, respectively. The thick portion of error bars are the clustered standard errors, and the thin portion of error bars shows 95%CIs. Other than the explanatory variables, estimation, subsampling, specification, and clustering approach remain identical to those in Table 2.